

SLAC - PUB - 3989
June 1986
T/AS

EVOLUTION OF COSMIC STRINGS II*

DAVID P. BENNETT[†]

Stanford Linear Accelerator Center

and

Physics Department,

Stanford University, Stanford, California, 94305

Submitted to *Physical Review D*

* Work supported by the Department of Energy, contract DE - AC03 - 76SF00515.

† Address after September 20, 1986: Theoretical Astrophysics Group, MS 209, Fermilab, P. O. Box 500, Batavia, IL 60510

ABSTRACT

The evolution of a system of cosmic strings is studied following an analytic model introduced by Kibble and developed in a previous paper. The properties of a scaling solution in the radiation dominated era are studied in detail, and it is shown that the conclusions of the previous paper are not sensitive to changes in the model for loop fragmentation. The scaling solution is also compared with the numerical results of Albrecht and Turok. A crude attempt is also made to mimic transient effects in the simulations, and the implications of these transients are discussed. The bound on the string tension due to primordial nucleosynthesis is discussed in some detail. The bound at present is $G\mu \lesssim 4 \times 10^{-6}$. The evolution of a string system is also studied in the matter dominated era and in the transition between radiation and matter domination. The results are summarized in a pair of analytic fits that describe the evolution of the string system through the transition.

1. INTRODUCTION

In a previous paper¹ (I), I presented an analytic treatment of the cosmological evolution of cosmic strings in based on a formalism introduced by Kibble.² The fate of a system of cosmic strings depends on a complicated energy loss mechanism that is presumed to allow the energy density in strings to scale like that of radiation. If there are no interactions between strings, then it is well known^{3,4} that the strings will rapidly come to dominate during the radiation dominated era. Small closed loops of string are harmless because they will oscillate and eventually decay away through gravitational radiation. The difficulty arises because when strings are formed, the majority of the strings are in the form of infinite strings which cannot radiate away. If we include interactions which allow strings to change partners when they cross, however, then the infinite strings can lose energy by the production of loops which will radiate away. It is generally assumed that, through the production of loops, the infinite strings will lose enough energy so that their density scales as $1/t^2$ just like the matter that dominates the universe. (Of course, the density in strings must be much smaller than the matter density.) Kibble² has shown that such a scaling solution can appear naturally as a stable fixed point of his string evolution equations. He has also shown that it is possible that such a scaling solution does not exist. In this case the energy density of the strings will come to dominate the universe at a very early time. This would rule out the cosmic string theory of galaxy formation which currently appears to be quite promising.⁵⁻¹³

The success of this scenario depends critically on the probability that, once formed, a loop will survive for a very long time without reconnecting to a long string. This is necessary because the gravitational radiation rate is very slow. In

(I), I showed that this requires that the “parent” loops which break off from the network of long strings must fragment into a large number of “child loops.” The fragmentation of the parent loops is important because large loops have a high probability to reconnect to the long strings. Whether the loop production rate and the fragmentation probability are large enough to allow a scaling solution can only be answered by numerical simulations of the detailed dynamics of strings. Preliminary indications from the simulation by Albrecht and Turok¹⁴ are that a scaling solution does exist. The fact that they also observe a high fragmentation probability lends credence to their result. However, these simulations have a fairly small dynamic range so the results will have to be confirmed if we are to have confidence that they are correct. The implications of the possibility that strings will come to dominate has been investigated by Kibble,¹⁵ but throughout most of this paper, I will assume that a scaling solution exists so that the strings will never dominate.

In this paper, the analysis presented in (I) will be extended in several ways. In Sec. 2, I briefly review the formalism developed in Ref. 2 and in (I), and I present a method for numerical evolution of the string evolution equations. The third section is devoted to the study of the scaling solution in the radiation dominated era. A simplified model of cosmic string evolution is used to point out an apparent inconsistency in the published numerical results of Albrecht and Turok. Their value for the number density of loops is shown to be inconsistent with the standard picture that loop production is the primary energy loss mechanism for the long strings unless the typical child loop size is very much smaller than that quoted from the numerical simulations.¹² It is suggested that this may be the result of deficiencies in their simulations, but several alternative explanations are

explored.

In Secs. 3.2 and 3.3, the properties of the scaling solution in a radiation dominated universe are studied as the various unknown parameters of the model are varied. A different model for the fragmentation of loops is also introduced and examined. Particular attention is paid to the dependence of the density of loops on these parameters because of the discrepancy mentioned above and because the bound on the string tension μ from primordial nucleosynthesis depends sensitively on this number. The results of this investigation are summarized in analytic fits that give the number density of loops as a function the density of long strings at the scaling solution, the loop reconnection suppression factor δ , and the probability of self-intersection p_{SI} . [In the case of the second loop production function, p_{SI} is replaced by the number of child loops, N_ℓ .]

One of the major results of (I) was a bound on the string tension μ obtained by limiting the density of gravitational radiation emitted by the loops to be consistent with the restrictions placed by the successful primordial nucleosynthesis scenario. The the energy density of the gravitational radiation emitted by the strings is larger than the energy density of the strings by a large logarithmic factor. The total energy density in gravitational radiation behaves gravitationally just like any other relativistic particle species so its density is limited to be less than 17% of the density of the known electrons, photons, and neutrinos at the time of nucleosynthesis.¹⁶ Unfortunately, in (I) I misquoted this number to be 8%. [This same mistake also appears in Refs. 17 and 18.] Since the gravitational radiation density is proportional to $\sqrt{G\mu}$, the correct bound is a factor of 4 weaker than the bound given in (I). The correct bound, as given in the Erratum to (I), is $G\mu \lesssim 4 \times 10^6$. [G is Newton's constant.] In this paper, the

derivation of this bound is discussed in somewhat more detail than in (I). The analytic fits for the loop density are used to give the bound on $G\mu$ as a function of the density of long strings, δ , and $p_{s,l}$. Changes in the bound due to different assumptions about particle physics and the underlying field theory of the strings are also discussed. It is also pointed out that this bound conflicts with recent claims^{19,20} that gravitational lenses with a separation of several arc minutes are a predicted consequence of cosmic strings.

Sec. 4 deals with the approach to the scaling solution from an initial condition similar to that used in the numerical simulations. The evolution equations are integrated numerically starting with an initial condition devoid of small loops in an attempt to mimic the approach to the scaling solution seen in the numerical simulations. It is shown that the string system approaches the scaling solution only fairly slowly, and it is argued that this may be a contributing factor to anomalously low value for the density of loops reported by Albrecht and Turok. In fact, it is noticed that for a non-negligible range of parameters, it is possible that the string system seems to approach a fictitious "scaling solution" on short time scales. Then, after a time much longer than the numerical simulations can run, the density in strings slowly begins to overtake that of radiation. This can occur when the rate of loop production is sufficient for a scaling solution when loop reconnection is neglected. Only after a large number of loops have been produced does loop reconnection become important, but when this occurs it interferes with loop production to such an extent that a scaling solution cannot be maintained. In order to rule out this unpleasant scenario it is necessary to obtain more detailed results from the numerical simulations.

The evolution of strings in the matter dominated universe is studied in Sec.

5. First, it is shown that the scaling solution in the matter dominated era has several differences from the solution in the radiation era. In the matter era, very little loop production is needed to prevent the strings from coming to dominate. Since we know that loop production must be copious in the radiation era, it is expected that energy loss from loop production will also be an effective energy loss process in the matter era. This means that there must be a great deal of string stretching to balance the energy loss to loop production. This in turn implies that the density in long strings will be a substantially smaller fraction of the total energy density in the matter era than in the radiation era. Unfortunately, the prediction of the actual number density of the long strings depends the behavior of the long strings when their curvature is close to the horizon size, so we will probably have to wait for numerical simulations in the matter dominated era to obtain this number. Once it is obtained, however, it may not be very difficult to describe the behavior of strings during the transition from the radiation era to the matter era. This is the main result of Sec. 5.2 in which the evolution equations are numerically integrated through the transition. It turns out that even though the transition takes much too long for a numerical simulation to follow it, the characteristics of the transition seem to be well described in terms of parameters that can be determined by the study of the scaling solutions in both the matter and radiation eras.

2. THE STRING EVOLUTION EQUATIONS

In this section, I review the formalism used to study the evolution of cosmic strings in (I), and I present a numerical method for solving these equations with arbitrary initial conditions and with a scale factor $R(t)$ that is an arbitrary function of time.

2.1 REVIEW

This formalism treats the production and reabsorption of closed string loops by a system of infinite (or long) strings. It is crucial to understand these processes because they control the fate of the string system. It is easy to show using simple dimensional arguments that we can always expect loop production to be efficient enough *if* we can neglect the reabsorption of loops by infinite strings. This is because we have a free parameter that controls the rate of loop production. The loop production rate is controlled by the ratio of the scale length of the system of infinite strings to the horizon size. By setting this ratio to be sufficiently small, we can increase the rate of loop production (with respect to the expansion rate) until it is sufficient for the existence of a scaling solution. Once we allow for loop reconnection, however, this argument no longer holds. Now, if we set the scale length of the string system to be much smaller than the horizon, the reconnection rate will also become very large. Thus, in this limit we expect the system of loops and infinite strings to reach a state resembling equilibrium with little or no net energy transfer between loops and infinite strings. Therefore, it is important to consider the reconnection process in detail.

In this formalism, the system of strings is divided into two classes: (1) long strings which include infinite strings and loops with a radius much larger than

the average separation between the strings, and (2) loops. The energy of the long strings in a comoving volume V is given by

$$E = \frac{\mu V}{L^2} , \quad (2.1)$$

This equation defines the scale length of the long string, L , which is roughly the average distance between strings. Without interactions, the equation for the time derivative of E in an expanding universe is,³

$$\dot{E} = E \frac{\dot{R}}{R} (1 - 2 \langle v^2 \rangle) , \quad (2.2)$$

where R is the scale factor, and $\langle v^2 \rangle$ is given by

$$\langle v^2 \rangle \equiv \int dx \frac{v^2}{\sqrt{1 - v^2}} \quad (2.3)$$

From (2.2) and (2.3) we can see how the energy density of the long strings will scale in several limiting cases. If the strings are moving at very small velocities, Eq. (2.2) tells us that the density in strings scales as $\rho_s \sim 1/R^2$ as we might expect. If the strings move at the speed of light, we see that $\rho_s \sim 1/R^4$ just like ordinary relativistic matter. Finally, if the scale length of the strings (L) is much smaller than the horizon, then it can be shown^{3,2} that $\langle v^2 \rangle = \frac{1}{2}$. So, in this case the density of strings scales as $\rho_s \sim 1/R^3$ like nonrelativistic matter. Turok and Bhattacharjee have shown that, with no interactions, $\frac{1}{2}$ is the maximum possible value for $\langle v^2 \rangle$ so that the density of a non-interacting system of strings must scale like $\rho_s \sim 1/R^n$ where $2 \leq n \leq 3$.

A realistic treatment of string evolution must include the interactions between the strings. In order to describe these interactions, we must know the probability that two segments of string will intercommute (change partners) when they

cross. In general, this will depend on the angle and the relative velocity of the crossing, but we will take the intercommuting probability (p) to be a constant. The question of the intercommuting probability for the simpler case of global strings has been studied by Shellard²¹ and he has found that the strings will intercommute in almost all cases. Therefore, I will usually take p to be 1. If the correct value for p is not 1, then the correct scaling solution can be obtained by rescaling γ such that p/γ remains fixed.

The size of a loop will be denoted by $x = \ell/L$ where ℓ is the proper radius of the loop. [This means that its energy is $2\pi\mu\ell$. The real radius of a loop is always smaller than ℓ .] The number density of loops with proper radii between ℓ and $\ell + d\ell$ is given by

$$n(\ell) d\ell = \frac{1}{2\pi\mu\ell} \frac{E}{V} f\left(\frac{\ell}{L}\right) \frac{d\ell}{L}, \quad (2.4)$$

so that the energy density in loops of size x to $x + dx$ is

$$\frac{E}{V} f(x) dx. \quad (2.5)$$

Note that in general $f(x)$ can have explicit time dependence, but at a scaling solution it will be time independent.

The most straightforward assumption to make in order to determine the interaction rate between strings is to treat the strings as a gas of uncorrelated string segments. This may not be too bad for the long strings, but it would clearly overestimate the probability that a loop will reconnect to a long string for the following reasons. For instance, when a long string collides with a small loop, it seems likely to collide with the loop at two points. This would mean that the loop is initially absorbed by the long string, but a second loop of roughly half

the size of the first would be produced by the second intercommutation. Also, a loop has a smaller cross section for a collision than an uncorrelated segment of the same length. These effects will be accounted for by including a factor $\delta < 1$ in front of the loop reconnection term in the evolution equations. We can expect each of the effects mentioned above to suppress reconnection by at most a factor of $\frac{1}{2}$ so we can expect that $\delta \geq 0.25$. Perhaps $\delta \approx 0.5$ is about right.

If we treat the systems of loops and long strings as uncorrelated segments (with the one correction for loop reconnection), then the string evolution equations can be derived,^{2,1}

$$\frac{L}{E} \frac{d}{dt} \left(\frac{E}{L} f(t, x) \right) = \frac{p\bar{v}}{L} (x a(x) - x\delta f(t, x)) + \frac{\dot{\ell}}{xL} f(x) , \quad (2.6)$$

$$\frac{\dot{E}}{E} = \frac{\dot{R}}{R} (1 - 2\langle v^2 \rangle) + \frac{p\bar{v}}{L} \int x [\delta f(t, x) - a(x)] dx , \quad (2.7)$$

where \bar{v} is an average velocity defined by

$$\bar{v} \equiv \pi \left\langle \max(v_1, v_2) \sqrt{1 - v_1^2} \sqrt{1 - v_2^2} \right\rangle . \quad (2.8)$$

v_1 and v_2 are the velocities of colliding segments.

Eq. (2.7) describes the long strings. It is obtained by adding interaction terms to (2.2). The integral on the right hand side of (2.7) describes the energy gain from loops and the energy loss from the long strings through loop production. Loop production is described by the loop production function, $a(x)$, which will be discussed in detail below. Eq. (2.6) describes the loops. The $\dot{\ell}$ term in the (2.6) is included to account for loop decay by gravitational radiation.^{22,23} I will

set

$$\dot{l} = -10 G\mu , \quad (2.9)$$

consistent with the results of Refs. 22 and 23. I have assumed that the loops under consideration are small enough so that $\langle v_{\text{loop}}^2 \rangle \approx \frac{1}{2}$, and the stretching of the loops can be neglected. Loops that are large enough so that this is not true should be included as long strings.

If we set $R = R_0 t^N$ and $L = \gamma t$ where R_0 and γ are constants, then we can attempt to find a scaling solution. Eq. (2.6) becomes

$$\begin{aligned} \frac{p\bar{v}\delta}{\gamma} x \left(f(x) - \frac{a(x)}{\delta} \right) &= \left(x + \frac{10 G\mu}{\gamma} \right) f'(x) \\ &+ 3(1 - N) f(x) - \frac{10 G\mu}{\gamma x} f(x) . \end{aligned} \quad (2.10)$$

The solution of (2.10) is

$$f(x) = \frac{p\bar{v}}{\gamma} \int_x^\infty dy a(y) e^{p\bar{v}\delta(x-y)/\gamma} \frac{x}{x+\epsilon} \left(\frac{y+\epsilon}{x+\epsilon} \right)^{3-3N+p\bar{v}\delta\epsilon/\gamma} , \quad (2.11)$$

where $\epsilon = 10G\mu/\gamma$. Substituting this into the long string equation, (2.7), we obtain

$$\begin{aligned} 0 = N(1 + \langle v^2 \rangle) - 1 + \frac{p\bar{v}}{2\gamma} \int_0^\infty dy a(y) \left[y \right. \\ \left. - \frac{p\bar{v}\delta}{\gamma} \int_0^y dx e^{p\bar{v}\delta(x-y)/\gamma} \frac{x^2}{x+\epsilon} \left(\frac{y+\epsilon}{x+\epsilon} \right)^{3-3N+p\bar{v}\delta\epsilon/\gamma} \right] , \end{aligned} \quad (2.12)$$

which is a constraint equation.

Eq. (2.12) can be used to find a scaling solution with the following procedure: First, we must input $\langle v^2 \rangle$ and \bar{v} as functions of γ . [In (I) it was argued that for $p \approx 1$, L should be the scale of curvature of the long strings as well as their mean separation. This implies that the velocities should be functions of γ .] Next, we must insert a loop production function $a(x)$ into (2.12) and adjust γ until (2.12) is satisfied. Kibble² has shown that in the radiation dominated era (2.12) will be satisfied by either no value of γ or by 2 values. In the former case, of course, no scaling solution exists while in the second case only the larger value of γ which satisfies (2.12) corresponds to a stable solution. If the initial value of γ is less than the lowest value which satisfies (2.12), then the system will evolve away from the scaling solution toward $\gamma = 0$. If the initial value is greater than the unstable solution of (2.12), then γ will approach the stable solution.

A somewhat different approach is probably better for finding scaling solutions given our limited knowledge of the loop production function. It is fairly easy to obtain an estimate for γ from the results of numerical simulations, but it is more difficult to compute the loop production function without a very careful analysis of the numerical results. Therefore, if we assume that a scaling solution does exist, it is more reasonable to fix γ to a value that seems to be consistent with the simulations and then compute the loop production normalization constant from the constraint equation, (2.12). This is the approach that is used in Sec. 3.

2.2 SOLUTION OF THE EVOLUTION EQUATIONS WITH ARBITRARY INITIAL CONDITIONS

In addition to the scaling solution, it is of interest to study the solution of (2.6) and (2.7) under conditions when a scaling solution would not apply. In

the period of transition between the radiation dominated era and the matter dominated era we would expect that the string system will transform from a radiation era scaling solution to a matter era scaling solution. However, there is no reason to expect that the strings will respond quickly to the change in the expansion law, so we must allow for departures from the scaling solution in the early part of the matter dominated era. This period is, of course, the most important time as far as galaxy and cluster formation is concerned, so it is important that it be understood.

Another application of the method developed in this section will be a test of the numerical simulations. Because we will be able to evolve (2.6) and (2.7) for an arbitrarily long time, we will be able to test the numerical simulations by starting with initial conditions similar to theirs and follow the string evolution for a long time. This will enable us to see whether the string system can really evolve to a scaling solution in the time available in the numerical simulations.

The main point of this numerical method is simply to note that the scale of the long string system (L) is a much more natural time than t . On the left hand side of (2.6) there will appear a term proportional to

$$\frac{d}{dt} \left(\frac{E}{L} f(t, x) \right) = \frac{\partial}{\partial t} \left(\frac{E}{L} f(t, x) \right) - \left(\frac{x E \dot{L}}{L^2} \right) f'(t, x), \quad (2.13)$$

where we have neglected the $\dot{\ell}$ term due to gravitational radiation because it only has a significant effect for very small loops (which only have a negligible effect on the evolution of the long strings). If I discretize L and x such that $L_{i+1}/L_i = x_{j+1}/x_j$ (for all i and j) then, the total time derivative in (2.13) can

be approximated by

$$\frac{d}{dt} \left(\frac{E}{L} f(t, x) \right) \simeq \frac{E_{i+1} L_{i+1}^{-1} f(t_{i+1}, x_j) - E_i L_i^{-1} f(t_i, x_{j+1})}{\Delta t}. \quad (2.14)$$

This formula treats the x dependence in eq. (2.13) exactly. Using (2.14) for the time derivative of $\frac{E}{L} f(t, x)$, (2.6) becomes

$$f(t_{i+1}, x_{j-1}) = \left(\frac{L_{i+1} R_i}{L_i R_{i+1}} \right)^3 \left[f(t_i, x_j) + \Delta t \frac{p\bar{v}_i}{L_i} x_j (a(x_j) - \delta f(t_i, x_j)) \right]. \quad (2.15)$$

$\Delta t = t_{i+1} - t_i$ is an unknown in (2.15), and it must be found from the discrete analog to (2.7) which is

$$\left(\frac{R_{i+1}}{R_i} \right)^3 \left(\frac{L_i}{L_{i+1}} \right)^2 = \left(\frac{R_{i+1}}{R_i} \right)^{1-2\langle v^2 \rangle_i} + \Delta t \frac{p\bar{v}_i}{L_i} \int x (\delta f(t_i, x) - a(x)) dx. \quad (2.16)$$

Since the relationship between R and t is given by an exact solution to Einstein's equations, (2.16) involves only a single unknown, Δt . Although (2.16) cannot be inverted to solve for Δt directly, an arbitrarily accurate approximate solution may be found by an iterative procedure. This allows us to find t as a function of L which can then be inserted into (2.15) to find $f(x)$.

3. PROPERTIES OF THE SCALING SOLUTION IN THE RADIATION DOMINATED ERA

In this section, the some of properties of the scaling solution, (2.11), will be explored. In (I), it was noted that, for many choices of parameters, the condition (2.12) cannot be satisfied and no scaling solution exists. Although *a priori* there is no compelling reason to assume that nature will have chosen the parameters so that a scaling solution does exist, I will assume that this is the case. There are two reasons for this. First, this seems to be the most interesting case (modulo Ref. 15), and second, a scaling solution seems to be indicated by the numerical simulations of Albrecht and Turok.¹⁴ In Sec. 3.1, I use a simplified model for string evolution to check some of the numerical results that have been quoted from the numerical results of Albrecht and Turok. Secs. 3.2 and 3.3 are devoted to studying the properties of the scaling solution as the various parameters of the model are varied. In Sec. 3.4, I study the primordial nucleosynthesis bound on $G\mu$ in some detail, and I show how it varies as a function of the parameters.

3.1 CHECKING THE NUMERICAL SIMULATIONS

In this section, I show that there is an apparent discrepancy between some of the published results of the numerical simulations and the analytic results presented here. Although this discrepancy can be seen from (2.11) and (2.12), the root of the problem is very simple, and it is more transparent to examine it in a simple model without the complexities of loop reconnection. Later, I will show that including the effects of reconnection generally tends to increase the discrepancy. I will assume that the density in long strings is

$$\rho_{LS} = A \frac{\mu}{t^2}, \quad A = 2.5 \pm 0.5, \quad (3.1)$$

which is the value quoted by Albrecht and Turok in Ref. 14. In Ref. 12, the number density of loops is given as

$$n(\ell) d\ell = \left(\frac{\beta}{2\pi}\right)^{3/2} \frac{\nu d\ell}{t^{3/2} \ell^{5/2}}, \quad (3.2)$$

with $\nu \approx 0.01$. The factor of $(\beta/2\pi)^{3/2}$ in (3.2) comes about because we have measured the loop size with the proper radius ℓ rather than the ordinary radius used in the simulations. The energy of a loop of radius r is denoted in Ref. 12 as βr with $\beta \simeq 9$. Thus, the relationship between ℓ and r is $2\pi\ell = \beta r$.

Now if there were no loop production, the energy density of the long strings would scale like nonrelativistic matter. Therefore, for a scaling solution we must have

$$\begin{aligned} \dot{\rho}_{LS} &= -3 \frac{\dot{R}}{R} \rho_{LS} - \dot{\rho}_{lp} \\ &= -4 \frac{\dot{R}}{R} \rho_{LS}, \end{aligned} \quad (3.3)$$

where $\dot{\rho}_{lp}$ represents the energy loss through loop production. Now we must make some model for the formation of loops. According to Ref. 12, the typical radius of the child loops is $0.2t$. Let us model loop production by assuming that in the time interval t to $t + dt$ the only (child) loops formed have radii between t/n_ℓ and $(t + dt)/n_\ell$ (where, following Ref. 12, we should expect that $n_\ell \simeq 5(2\pi/\beta) \simeq 3.5$). The reconnection of loops to long strings will be ignored.

This assumption allows us to make a simple connection between eq. (3.3) and eq. (3.2) which will allow us to relate ν and n_ℓ . Inserting expression (3.1) into (3.3), we obtain

$$\frac{A\mu dt}{2t^3} = d\rho_{lp}. \quad (3.4)$$

But $d\rho_{lp} = 2\pi\ell\mu n(\ell) d\ell$ for loops of size t/n_ℓ since no loops of this size existed before time t . Substituting $\ell = t/n_\ell$, we obtain

$$\frac{A\mu dt}{2t^3} = \frac{\beta^{3/2} n_\ell^{1/2} \nu \mu dt}{\sqrt{2\pi} t^3}, \quad (3.5)$$

or

$$\nu \geq \frac{1}{10.8 n_\ell^{1/2}} \left(\frac{9}{\beta}\right)^{3/2}, \quad (3.6)$$

where we have used $A \geq 2$. So, we must take $n_\ell \gtrsim 90$ to obtain $\nu = 0.01$, while $n_\ell = 3.5$ corresponds to $\nu \geq 0.05$ which is consistent with values obtained from the more sophisticated model described by (2.11) and (2.12). Clearly, there is a significant discrepancy here. It should be emphasized that the source of this discrepancy is *not* that I have claimed that $\nu \geq 0.1$ as is stated in Ref. 18. I make the claim that $\nu \geq 0.03(9/\beta)^{3/2}$ which is consistent with $n_\ell \leq 10$

The reader may wonder if it is possible that this discrepancy will disappear if some of the simplifying assumptions used above are dropped. Perhaps by including loop reconnection or using a different spectrum for the child loops, a lower value for ν could be obtained. This seems unlikely because loop reconnection tends to make the energy loss process less efficient and result a larger density of loops. Also, if we let the child loops have different sizes, the tendency is also to increase the value of ν . These questions will be studied further in Sec. 3.3 where the properties of the scaling solution will be investigated in detail.

Another possible source of the discrepancy between the numerical results and the simple model is the possibility that the numbers quoted from the numerical simulations may not represent the actual scaling solution values. For example, the value of $\nu \simeq 0.01$ was measured at $t = 3t_0$, and it is not clear that ν would

have reached its scaling solution value in such a short time. Furthermore, the density in long strings is likely to converge to its scaling solution value faster than the loop density, so there is no reason to expect that ν has reached its scaling solution value just because γ has. These questions will be investigated in more detail in Sec. 4 where I have attempted to reproduce the time dependent results of the simulations by evolving (2.15) and (2.16) from an initial condition similar to that used by Albrecht and Turok. We will see that the time it takes for the system to relax to the scaling solution may be longer than the time that Albrecht and Turok have allowed the simulation to run. This can contribute to the discrepancy between the analytic results and the numerical ones. In some cases, it is even possible that an apparent “scaling solution” seen on short time scales can disappear at later times.

Recently, I have been informed by the authors of Ref. 14 that several improvements have been made in their program. A few runs have been made with this improved version. The preliminary results²⁴ are that $\beta \simeq 15$ with $\nu \approx 0.01$. This new value for β would significantly lessen the discrepancy except that their value for A (see eq. (3.1)) is now $A \approx 3$ or 4. So the discrepancy has not yet been resolved. Turok has suggested that the resolution of the discrepancy may lie in the possibility that there is significant loop production at small loop sizes ($\sim 0.01t$). Unfortunately, the preliminary data from the new simulations is not yet sufficient to test this hypothesis, so we will have to wait and see.

3.2 THE LOOP PRODUCTION FUNCTION

In order to understand the solutions to (2.11) and (2.12) it is important to understand how they depend on the loop production function $a(x)$ and to know what types of loop production functions are reasonable. In (I) it was shown that a limit on the total integral of $a(x)$ can be obtained by assuming that the segments of the long strings that collide and intercommute can be regarded as uncorrelated. The limit is

$$F_\ell = \int a_p(x) dx, \quad F_\ell < 1, \quad (3.7)$$

where F_ℓ is the fraction of long string intercommutings that produce new loops. Even if the assumption that the long strings behave like uncorrelated segments is not very good, it is very likely that $F_\ell < 1$ anyway. The subscript "p" has been added to the loop production function to indicate that this bound applies to the loop production function for parent loops only. The distinction between parent loops and child loops is made because the rate of collisions between long string segments clearly cannot fix the rate of child loop production. This must certainly depend on the probability that the parent loops self-intersect.

As was argued in (I), the loop fragmentation process has critical importance for the evolution of the string system. This simplest way to include the fragmentation process is directly in the loop production function. The model for loop fragmentation presented in (I) assumed that a loop has a constant probability p_{SI} to split up into two equal sized pieces. p_{SI} was assumed to be a constant independent of loop size or "generation." This led to the definition

$$a_1(x) = A_n x^n \theta(\xi - x), \quad \xi \sim 1 \quad p_{SI} = \left(\frac{1}{2}\right)^{n+2}. \quad (3.8)$$

In order to relate $a_1(x)$ to F_ℓ , I have chosen a form for $a_p(x)$,

$$a_p(x) = \frac{F_\ell}{\ell n 2} \frac{1}{x} \theta(x - \xi/2) \theta(\xi - x), \quad \xi \sim 1. \quad (3.9)$$

Energy conservation implies that

$$\int_0^\infty x a_p(x) dx = \int_0^\infty x a_1(x) dx,$$

so

$$A_n = \frac{n+2}{2\ell n 2} \xi^{-n-1} F_\ell. \quad (3.10)$$

Another model for loop fragmentation has been suggested by Turok.²⁴ He has suggested that a parent loop fragments in such a way that all the resulting child loops have approximately the same size. This can be modeled by a loop production function of the form

$$a_2(x) = N_\ell F_\ell \delta\left(x - \frac{1}{N_\ell}\right), \quad (3.11)$$

where N_ℓ is the number of child loops produced assuming the typical (proper) radius of a parent loop is L . [If the typical parent loop size is different from this, then it is best just to take $1/N_\ell$ as the typical size of a child loop.] Note that if the reconnection of loops is neglected, this will reduce to the simpler model introduced in Sec. 3.1 with $N_\ell = \gamma n_\ell$.

The rationale for introducing the second loop production function is to test how string evolution depends on the shape of the loop production function. The loop production functions $a_1(x)$ and $a_2(x)$ are ideal for this because they represent

the opposite extremes of the possible shapes for the function (given that we must have a variable to describe the fragmentation of the parent loops). The function $a_1(x)$ is independent of scale (except for the size of the parent loops) producing child loops on all scales smaller than L while $a_2(x)$ represents the opposite extreme. The loop production function that describes the real evolution of the string system is likely to be “intermediate” between the two. Therefore, we should expect that any conclusions that hold for both of these loop production functions will hold for the real loop production function as well.

3.3 PARAMETER DEPENDENCE OF THE SCALING SOLUTION

In this section, we will study the scaling solution under the variation of the input parameters. I will take γ (the scale length of the long string system) to be an independent variable and F_l to be a dependent one that is fixed by the constraint equation (2.12). A convenient variable with which to describe the density of small loops is

$$\sigma = x^{3/2} f(x) . \quad (3.12)$$

From (2.11) it can be seen that $f(x) \sim x^{-3/2}$ over most of its range so that σ will vary only very slowly with x . Another advantage of this notation is that σ is independent of γ to a very good approximation.

Assuming that σ is approximately a constant, (2.4) can be used to calculate the total density of strings at the scaling solution. [If I use $\sigma(x = 0.01)$ as the “constant” value for σ , this gives ρ_s to better than 5%.] Expressed as a ratio to

the total density of relativistic matter the density in strings is given by

$$\begin{aligned}
\frac{\rho_s}{\rho_{rm}} \equiv \eta &= \left(\frac{3}{32\pi Gt^2} \right)^{-1} \left(\frac{\mu}{\gamma^2 t^2} \right) \int dx \frac{\sigma}{x^{3/2}} \\
&\simeq \frac{128\pi}{9\sqrt{10}} \frac{\sigma}{\gamma^{3/2}} \sqrt{G\mu} \\
&\simeq 14.1 \frac{\sigma}{\gamma^{3/2}} \sqrt{G\mu},
\end{aligned} \tag{3.13}$$

where I have used $\epsilon = 10G\mu/\gamma$. To obtain the result in eq. (3.13), I have included a factor of 2/3 which is the result of using (2.11) for the behavior of $f(x)$ at small x rather than taking $f(x) \sim x^{-3/2}$ and inserting ϵ as the lower limit of the integral. The relation between σ and the parameter ν used by Albrecht and Turok is

$$\nu = \frac{\sqrt{2\pi}}{\beta^{3/2}} \frac{\sigma}{\gamma^{3/2}}. \tag{3.14}$$

In Figs. 1 and 2, I have plotted σ vs. the loop size $\ell/t = \gamma x$. The different graphs in Figs. 1 and 2 correspond to different values of the loop production function parameters $p_{s\ell}$ and N_ℓ . For all the graphs, I have fixed the density in long strings to be $\rho_{Ls} = 2.5\mu/t^2$ (or $\gamma = 1/\sqrt{2.5}$) which is the value reported by Albrecht and Turok.¹⁴ $\langle v^2 \rangle$ has been taken to be

$$\langle v^2 \rangle = \frac{1}{2} \left(\frac{1}{1 + k\gamma^4} \right)^2, \tag{3.15}$$

as in (I) with $k = 1/16$. In the radiation dominated era, it is probably a good approximation that $\langle v^2 \rangle \approx \frac{1}{2}$. Hence, the value of k and the exact form of (3.15) are not very important here.

The sharp cusp that appears in the graphs of Fig. 2 is a somewhat unnatural artifact of the delta function loop production function. The curves in Fig. 2 decrease monotonically after the cusp as a result of the absorption of loops by the long strings. This is in contrast to the lower curves in Fig. 1 in which σ does not begin to decrease until $\ell/t \sim 10^{-3}$. For large values of p_{SI} , there is substantial loop production even for the smallest values of ℓ , and it is only the effect of the gravitational decay of loops that makes σ decrease for small ℓ .

Another difference between the two loop production functions can be seen in Fig. 3. In this figure, I have plotted the “loop production efficiency” vs. the probability of self-intersection p_{SI} for both the loop production functions, $a_1(x)$ and $a_2(x)$. [As before, I have fixed $\gamma = 1/\sqrt{2.5}$, $k = 1/16$ and $\xi = 1.5$.] The “loop production efficiency” is defined to be the fraction of the loops that break off from the long strings that do not eventually reconnect to the long string network. In order to plot the efficiencies for both the loop production functions on the same graph, it was necessary to assign a value of \tilde{p}_{SI} for each value of N_ℓ . Note that p_{SI} is a variable defined only in the context of $a_1(x)$ not $a_2(x)$. For the purpose of Fig. 3, I have defined $\tilde{p}_{SI}(N_\ell)$ to be the value of p_{SI} that gives a median loop size of $1/N_\ell$. Thus, as in (I), we have

$$\tilde{p}_{SI} = 2^{-\ln(N_\ell)/2} . \quad (3.16)$$

[The curves in Fig. 3 terminate when p_{SI} becomes small because no scaling solution exists for these values.]

A couple of the main features of Fig. 3 have already been discussed in (I): namely that the efficiency of loop production can be increased by either increasing the self-intersection probability or by decreasing δ . Now, we can also see that

the form of the loop production function also affects the efficiency. For a fixed median loop size we see that the efficiency of loop production function $a_2(x)$ (the δ function) is generally about 20% larger than that for $a_1(x)$. Because the function $a_1(x)$ produces child loops of all sizes, it will give a large fraction of child loops that are close to the horizon size which will be likely to be absorbed by the long strings. Thus, producing all the child loops of the same size is the most efficient way for the long strings to lose energy.

The scaling solution depends on several other parameters in addition to the probability of self-intersection and the form of the loop production function. These parameters include γ , $\langle v^2 \rangle$, ξ (see (3.8)) and δ , the suppression factor for loop absorption by the long strings. In this paper, I will set $\xi = 1.5$ and ignore any possible variation of this parameter on the grounds that my results will be qualitatively the same with any value for ξ , and that in order to change ξ enough to make a significant change in any of my numerical results I must assume that the radius of the parent loops is very different than the average separation between the long strings.

In this section, I will take $\langle v^2 \rangle$ to be given by (3.15) with $k = 1/16$. This gives $\langle v^2 \rangle \simeq \frac{1}{2}$ which is probably about right. If the true value of $\langle v^2 \rangle$ is different from what I have assumed, then my value for σ can be corrected with the following formula

$$\sigma = \frac{1 - \langle v^2 \rangle}{1 - \langle v_0^2 \rangle} \sigma_0, \quad (3.17)$$

where the 0 subscript indicates the values I have obtained with my assumptions. $\langle v^2 \rangle$ cannot be larger than $\frac{1}{2}$ unless the interactions between the long strings cause the string system to become much more bumpy than a random walk. More

likely is the possibility that $\langle v^2 \rangle \lesssim \frac{1}{2}$. [This seems to be what the numerical simulations find.] In this case, the long strings will gain energy by stretching according to (2.2). This energy must be lost through loop production, so that the number of loops produced would have to be increased over what I have assumed here. Thus, if $\langle v^2 \rangle < \frac{1}{2}$, then $\sigma > \sigma_0$. This would make the discrepancy with the numerical simulations even larger.

The variation of the scaling solution with γ , and to some extent δ can be treated very simply by noting that σ is almost independent of these variables when they are in the range of interest. For the case when the loop production function is a delta function (eq. (3.11)), it is not difficult to show that this is true. Let us insert the loop production function, (3.11), into the constraint equation (2.12), and solve for F_ℓ . To first order in δ/N_ℓ we obtain,

$$F_\ell \simeq \frac{\gamma}{p\bar{v}} \frac{1 - \langle v^2 \rangle}{1 - 2 \frac{p\bar{v}\delta}{\gamma N_\ell}}. \quad (3.18)$$

Inserting this value for F_ℓ into (2.11) and (3.12), we find that

$$\begin{aligned} \sigma &\simeq \frac{1 - \langle v^2 \rangle}{N_\ell^{1/2}} \frac{e^{p\bar{v}\delta(x-1/N_\ell)/\gamma}}{1 - 2 \frac{p\bar{v}\delta}{\gamma N_\ell}} \\ &\simeq \frac{1 - \langle v^2 \rangle}{N_\ell^{1/2}} \left(1 + \mathcal{O} \left(\frac{p\bar{v}\delta}{\gamma N_\ell} \right) \right). \end{aligned} \quad (3.19)$$

Thus, when δ/N_ℓ is small, σ is almost constant. Variation of σ is further suppressed by the fact that we are generally interested in only a small range of the possible values for γ . The numerical simulations seem to indicate that $2 < 1/\gamma^2 < 4$. Thus, even if we take N_ℓ to be as small as 2, σ varies by only 6% when we change γ from the value $1/\sqrt{2.5}$ that was used above to 0.5. If $N_\ell = 5$, then we can allow γ to be as small as $1/3$ without changing σ by more than 10%.

Although, I have shown that σ is insensitive to γ only for the delta function loop production function, it is true to almost the same accuracy for the power law loop production function, $a_1(x)$. Unfortunately, there is not such a simple argument to show that this is the case, but explicit calculation confirms that it is true to 5% or better. Only, when $p_{SI} > 0.95$ or $p_{SI} < 0.55$ does this relationship begin to break down.

The values of σ as a function of δ and p_{SI} or N_ℓ are summarized in Table 1. This gives the results of an analytic fit to my numerical evaluation of σ which was calculated from (2.11), (2.12) and (3.12). If we combine these formulas with eqs. (3.13) and (3.14), we can calculate the energy density of the string system or Albrecht and Turok's number density parameter ν directly from the input parameters. The accuracy of this procedure is usually about 5% or better and almost always better than 10%.

loop production function	δ	σ	error	range of validity
$a_1(x)$	0.5	$1.31(1 - p_{SI})^{1.03}$	$\lesssim 3\%$	$p_{SI} > 0.5$
$a_1(x)$	0.3	$1.11(1 - p_{SI})^{0.94}$	$< 2\%$	$p_{SI} > 0.35$
$a_1(x)$	0	$0.76(1 - p_{SI})^{0.76}$	$\lesssim 7\%$	$p_{SI} > 0.35$
$a_2(x)$	0.5	$0.78 N_\ell^{-0.64}$	$\lesssim 5\%$	$40 > N_\ell > 2$
$a_2(x)$	0.3	$0.65 N_\ell^{-0.58}$	$\lesssim 4\%$	$40 > N_\ell > 1.5$
$a_2(x)$	0	$0.5 N_\ell^{-0.5}$	exact	

Table 1. Fits for σ as a function of δ and p_{SI} or N_ℓ .

With the results summarized in Table 1, we can now see how the discrepancy

discussed in section 3.1 is modified when we include the effects of loop reconnection. In general, including the reconnection process by setting $\delta \neq 0$ gives larger values for σ and ν , so it makes the discrepancy with the numerical simulations worse. In fact, with loop production function $a_2(x)$, it can be shown that σ is a monotonically increasing function of δ . To lowest order in δ/N_ℓ , this is clear from (3.19). A more general argument can also be given. From the argument given in section 3.1 it is clear that the density in small loops must be proportional to the density in long strings. However, loops that will eventually reconnect behave essentially like long strings because they will not ever become small enough (with respect to the horizon) to radiate efficiently. Thus, increasing δ has the effect of increasing ρ_{LS} which results in a proportionate increase in σ and ν .

For large values of N_ℓ or p_{SI} , this argument seems to contradict the results listed in Table 1. For $a_2(x)$, this is just due to the errors in the fits, but for $a_1(x)$ with a large value for p_{SI} , σ does begin to decrease for large values of δ . This can happen for $a_1(x)$ because the child loops are produced at all sizes. Since the larger loops are preferentially reabsorbed by the long strings, increasing δ can have the effect of increasing the proportion of small loops that are produced. For $\delta \leq 0.5$, this effect only dominates when $p_{SI} \gtrsim 0.85$, and even then it is a small effect.

3.4 THE NUCLEOSYNTHESIS CONSTRAINT

In (I), I presented a simple argument to show that the bound on the density of unknown particles that comes from primordial nucleosynthesis¹⁶ can provide a stringent limit on the cosmic string theory of galaxy formation. [This constraint was found independently by Davis.¹⁷] Without gravitational radiation the energy

density in strings would scale as $1/R^3$ because the energy density is dominated by small loops which behave just like nonrelativistic matter. In a scaling solution (when the universe is dominated by relativistic matter) $\rho_s \sim 1/R^4$, so the difference between $\rho_s \sim 1/R^3$ and $\rho_s \sim 1/R^4$ must be the energy density emitted in gravitational radiation. This means that the strings radiate a large fraction of their energy density into gravitational radiation in each expansion time. Thus, the total density of gravitational radiation is larger than the energy density in strings by the factor $\ln(t/t_0)$ where $t_0 = m_p^3/\mu^2$ is the time when the strings begin to evolve freely.²⁵ Since the density in strings is of the order of a few tenths of a percent of the density of relativistic matter (a few $\times \sqrt{G\mu} \rho_{rm}$), and since $\ln(t/t_0) \sim 60$ at the time of nucleosynthesis, the energy density of gravitational radiation is likely to be close to the upper bound provided by nucleosynthesis. [The upper bound is 17% of the density of the known relativistic matter.¹⁶]

Here, I present a more detailed argument taking into account the change in the expansion law when various particle species go nonrelativistic and annihilate as well as the slight change in the expansion due to the presence of strings. Let us assume that at t_0 energy density in relativistic matter is given by

$$\rho_{rm}(t_0) \equiv \rho_0 = \frac{3}{32\pi G t_0^2}, \quad (3.20)$$

and that the string density is

$$\rho_s = \eta \rho_0 \frac{t_0^2}{t^2} \quad (3.21)$$

where η is the ratio of the string density to the relativistic matter density introduced in eq. (3.13). Initially $\rho_{gr} = 0$, and then it is evolved according to

$$\dot{\rho}_{gr} = \frac{\dot{R}}{R} \rho_s - 4 \frac{\dot{R}}{R} \rho_{gr}. \quad (3.22)$$

Eqs. (3.20), (3.21), and (3.22) can be used with the Friedmann-Robertson-Walker version of Einstein's equation to yield the following solution:

$$\begin{aligned}
 R &= R_o \left(\frac{t_o}{t} \right)^{\frac{1}{2} + \frac{\eta}{8}} \\
 \rho_{rm} &= \rho_o \left(\frac{t_o}{t} \right)^{2 + \frac{\eta}{2}} \\
 \rho_{gr} &= \rho_s \frac{1 + \frac{\eta}{4}}{\eta} \left(1 - \left(\frac{t_o}{t} \right)^{\frac{\eta}{2}} \right) .
 \end{aligned} \tag{3.23}$$

The quantity that is limited by nucleosynthesis is the total density of strings and gravitational radiation divided by the density in ordinary relativistic matter. From (3.23) this is given by

$$\frac{\rho_s + \rho_{gr}}{\rho_{rm}} = \eta \left(\frac{t}{t_o} \right)^{\frac{\eta}{2}} + \left(\frac{t}{t_o} \right)^{\frac{\eta}{2}} - 1 , \tag{3.24}$$

where the first term on the right hand side is the contribution from ρ_s and the last two terms come from ρ_{gr} .

Eq. (3.24) is still incomplete because the effects of annihilation of the massive particle species has not been included. This will have a negligible effect on the string term because the strings will adjust themselves to stay in a scaling solution with the same fraction of the total energy density both before and after the transition. The annihilation will have a non-negligible effect on the density of gravitational radiation because the universe expands slightly faster during the transition so that the gravitational radiation emitted before the transition will be redshifted. The change in ρ_{gr}/ρ_{rm} is given by $(g_{i+1}/g_i)^{1/3}$ where g_i and g_{i+1} are the effective number of particle species before and after the transition.²⁶ [For

the purpose of calculating g_i , a fermion counts as 7/8 of a boson.] With the annihilation correction factors, (3.24) becomes

$$\begin{aligned} \frac{\rho_s + \rho_{gr}}{\rho_{rm}} = & \eta \left(\frac{t}{t_o} \right)^{\frac{\eta}{2}} + \left(\frac{g_n}{g_o} \right)^{\frac{1}{3}} \left(\left(\frac{t_1}{t_o} \right)^{\frac{\eta}{2}} - 1 \right) + \dots \\ & + \left(\frac{g_n}{g_i} \right)^{\frac{1}{3}} \left(\left(\frac{t_i}{t_n} \right)^{\frac{\eta}{2}} - 1 \right) \dots \end{aligned} \quad (3.25)$$

Note that the t_i values that occur in (3.25) should be later than the time of the appropriate phase transition by a factor of about 10^4 because this is roughly the amount of time it takes before the loops that were formed at the phase transition to begin to dominate the string energy density and the production of gravitational radiation. Eq. (3.25) can be used to calculate $(\rho_s + \rho_{gr})/\rho_{rm}$ as a function of η . By requiring $(\rho_s + \rho_{gr})/\rho_{rm} < 0.17$, an upper bound on η can be found. (3.23) can then be used in combination with Table 1 to obtain an upper bound on $G\mu$ as a function of the input parameters: γ , δ , and p_{SI} or N_ℓ .

time (sec.)	g_i
10^{-31} to 2×10^{-11}	106.75
Weinberg-Salam transition, $T = 100$ GeV	
2×10^{-11} to 2×10^{-10}	96.75
top quark mass (?) $T = 40$ GeV	
2×10^{-10} to 10^{-8}	86.25
bottom quark mass, $T = 5$ GeV	
10^{-8} to 7×10^{-8}	75.75
tau & charm mass, $T = 2$ GeV	
7×10^{-8} to 3×10^{-6}	61.75
QCD transition, $T = 300$ MeV	
3×10^{-6} to 6×10^{-5}	14.25
muon mass, $T = 100$ MeV	
6×10^{-5} to 1	10.75
nucleosynthesis starts, $T = 1$ MeV	

Table 2. Values of g_i .

In order to obtain bounds on $G\mu$, it is necessary to make some assumptions about the value of g at times before the Weinberg-Salam phase transition. The values for g_i that I have used are given in Table 2. I have assumed that there are no new particles with a mass less than about 10^{13} GeV which is the temperature when the strings begin to move freely. This minimizes the dilution of ρ_{gr} that occurs when g_i changes and leads to the strongest possible bound on $G\mu$. These values of g_i give the bound $\eta < 0.0092$ which is used to obtain Figs. 4 and 5. A more conservative assumption would be that $g \gg 100$ for $T > 1$ TeV so that a significant amount of gravitational radiation would not start to build up before

then. In this case, I obtain $\eta < 0.0171$ which weakens the bounds in Figs. 4 and 5 by a factor of 3.5. The weaker bound could also apply in some of the more exotic cosmic string models in which the Higgs potential is very flat. With a very flat potential, the Higgs can get a very large expectation value even with a small mass term. Thus, strings with $G\mu \sim 10^{-6}$ could conceivably form at the Weinberg-Salam transition. Very flat potentials seem to occur in superstring theories compactified on Calabi-Yau manifolds,²⁷ but these potentials are not flat enough to give strings with $G\mu \sim 10^{-6}$ that form at the weak scale.

The upper bound on $G\mu$ is plotted as a function of p_{SI} and $1/\gamma^2 = \rho_{LS} t^2 / \mu$ in Fig. 4 and as a function of N_ℓ and $1/\gamma^2$ in Fig. 5. The finite thickness of the curves in 4 and 5 corresponds to varying δ between 0.3 and 0.5. $\delta = 0.5$ provides the more stringent limit on $G\mu$ except in Fig. 4 for $p_{SI} > 0.85$ in which the opposite is the case. The shaded lines in the figures indicate the regions of parameter space that seem to be excluded by the numerical simulations. The allowed regions are $1/\gamma^2 > 2.0$, and $p_{SI} < 0.85$ or $N_\ell < 10$. These bounds are intended to be conservative estimates; the actual values may imply a more stringent bound on $G\mu$. The bound implied by these assumptions is $G\mu < 4 \times 10^{-6}$ in the case of a “desert” between 100 GeV and 10^{13} GeV or $G\mu < 1.4 \times 10^{-5}$ in the more conservative case where all the radiation for $T > 1$ TeV is neglected.

One factor that has not been included in the bounds on $G\mu$ is that some of the string energy goes into the kinetic energy of loops which is subsequently redshifted away. If I use the result from the numerical simulations that $v_{loop} \lesssim 0.2$ then this will only reduce the bound on $G\mu$ by about 4%.

Finally, I would like to emphasize that the nucleosynthesis bound contradicts recent claims that gravitational lenses with image separations of several arc

minutes are a predicted consequence of cosmic strings.^{19,20} These claims have recently received a lot of attention due to the lens candidate with a 2.6' image separation reported by Turner *et. al.*²⁸ Although subsequent observations now suggest that the quasar pair is not lensed,²⁹ it should be pointed out that if such an object existed it could not be easily explained as a cosmic string. The typical separation of the images of an object that is lensed by a cosmic string³⁰⁻³² is $4\pi G\mu$, so 2.6' corresponds to $G\mu \sim 6 \times 10^{-5}$ an order of magnitude above the nucleosynthesis bound. Values of $G\mu$ greater than 10^{-5} are also in disagreement with measurements of the microwave background anisotropy³³ as well as estimates of $G\mu$ from galaxy and cluster formation arguments.^{12,13}

4. RELAXATION TO THE SCALING SOLUTION

In the preceding sections, I have concentrated on the properties of scaling solutions and studied those properties under a wide range of assumptions regarding the various parameters that characterize the analytical model. I have assumed that the evolution of the string system in the radiation dominated era is in fact described by a scaling solution, but the evolution of a real system of strings will depend on the initial conditions. It is known that if the initial value of γ is not too small,² then the string system will evolve toward a scaling solution (if such a solution exists), but it is not yet clear how quickly the scaling solution will be reached. Since the strings have been evolving freely since $t_0 \sim 10^{-31}$ sec., it is extremely unlikely that a scaling solution would not have been reached by any time of interest for the galaxy formation.

A more realistic concern is that the time it takes a string system to reach a scaling solution is long compared to the length of time that it is practical to run

numerical simulations. The simulations done by Albrecht and Turok started with only 20% of the initial string length in the form of loops, whereas in a scaling solution the density is dominated by small loops. Since they are only able to run for a short time before the horizon grows to be as large as their whole box, it is important to ask whether any of their results could be an artifact of their initial conditions.

The most important question is, of course, whether their “scaling solution” could be an artifact of their initial conditions, but even if it is not an artifact, it seems to be quite plausible that the lack of small loops in their initial state may be responsible for their apparent underestimate for ν . In the runs in which they attempt to measure ν , they start with an initial separation of strings that is roughly the same as that which they see in their “scaling solution.” They then only run for a factor of 3 in time³⁴ before they measure ν . Since their initial condition had few small loops, it is quite possible that their value for ν is not the scaling solution value. Because the reconnection of small loops is suppressed, a large error in ν would not imply that there is a similar error in the energy density of the long strings.

In (I), I integrated (2.6) and (2.7) numerically in order to test the validity of Albrecht and Turok’s main conclusion: that a scaling solution exists. I found that with initial conditions similar to those used by Albrecht and Turok, it is indeed possible that the strings will initially seem to evolve toward a scaling solution and then grow to dominate the universe once a large number of loops have been produced. However, I argued that this scenario is only possible when the parameters of the model are fine tuned to be close the values which allow a scaling solution. With, the improved numerical method presented here, however,

I have been able to do a better test of this scenario, and I have found that the tuning required for this scenario is not so fine.

The numerical calculations in (I) were done very crudely, and the numerical methods used gave rise to instabilities that limited the integration to a factor of 20 or 30 in time. The method used here as described by eqs. (2.15) and (2.16) is completely stable, and can be integrated for an arbitrarily long time.

In order to imitate the numerical simulations, eqs. (2.15) and (2.16) were evolved from an initial state with no small loops, *i. e.* $f(x) = 0$. This may seem to be a slight exaggeration of Albrecht and Turok's initial conditions since they start with 20% of the initial string length in loops; however, it should be recognized that this 20% percent includes all loops of size greater than or equal to the scale length whereas I include loops of size larger than the scale length with the long strings. In any event, the comparison between my results and the numerical simulations should only be taken to give a qualitative description of the magnitude of the errors that may occur in the numerical simulations.

The results of one of my numerical calculations are summarized in Figs. 6, 7, 8, and 9. These graphs show the results of several separate calculations with $\delta = 0.5$, $\xi = 1.5$ and $k = 1/16$ with the initial condition $f(t_0, x) = 0$. Fig. 6 is an example of the approach to a scaling solution from this initial state with $p_{sl} = 0.81$ and $F_l = 0.47$. It shows how the density in loops changes with time. σ/γ^2 is plotted here rather than σ in order to include the γ dependence of the loop density. The first curve in Fig. 6 corresponds to $t = 1.5t_0$, and the subsequent curves each correspond to about a factor of 8 later than the previous one. The behavior of the string system can be easily understood from this figure and Fig. 7(a) which gives $1/\gamma^2$ (or $\rho_{LS}t^2/\mu$) as a function of time. Initially there

are no loops, and the density of the long strings begins to drop, quickly losing energy through the production of loops. By about $t \approx 20t_o$ (the third graph in Fig. 6) a sufficient number of loops have been produced so that the absorption of loops by the long strings halts the decrease in the density of the long strings. Now, the absorption process begins to dominate slightly and the density in long strings starts to grow slowly. This growth is also reflected in the loop density which now grows slowly due to increased loop production by the long strings. By about $t \approx 10^4 t_o$, the smallest loops reach 10^{-6} times the horizon size and disappear off the end of the graph. [If I had included the gravitational radiation terms in (2.15) and (2.16), then these graphs would taper off at small ℓ/t just like the graphs in Figs. 1 and 2.] For the rest of the run (until $t = 10^{15} t_o$), the energy density in both the long strings and the loops increase slowly toward their scaling solution values.

If I had chosen different parameters the time dependent solution would be qualitatively the same as long as I keep $p_{sI} \geq 0.7$. If the typical child loop size is about one tenth of the typical parent loop size,¹¹ then the correct value for p_{sI} is about 0.80 ± 0.05 . However, the value $1/10$ for the size of the child loops is just an estimate, so we should not restrict ourselves to $p_{sI} \geq 0.7$. In (I), I argued that if $p_{sI} < 0.7$, a scaling solution is not guaranteed; depending on the values of F_ℓ and δ , a scaling solution may or may not exist. This would not necessarily be a problem except that for certain values of F_ℓ and δ , it is possible that the numerical simulation will see a transient that will mimic evolution toward a scaling solution. At early times, the string system would evolve in a way very similar to the approach to the scaling solution shown in Figs. 6 and 7(a), so when the simulations terminate, it appears that the string system has reached

a scaling solution. Only if the simulations could be run a good deal longer would the transient disappear and the string density begin to grow. Thus, if the correct value of p_{sI} is in this range, it is possible that a scaling solution does not exist and that the main conclusion of Albrecht and Turok is entirely spurious. If this scenario is correct, it indicates that the loop production rate would be sufficient for a scaling solution if there was no reconnection. Once a sufficient density of loops builds up, however, reconnection becomes important, and the loop production rate is no longer sufficient. In (I), I suggested that this scenario was possible, but that it would only occur when the parameters have been fine tuned. My most recent calculations show that this is not the case; this type of transient occurs for a non-negligible range of parameters.

Fig. 7 shows the behavior of the density of long strings ($1/\gamma^2$) as a function of time. Curve (a) is from the same calculation as Fig. 6, my scaling solution example. Note that although $1/\gamma^2$ starts at its scaling solution value of 3.5, it quickly drops to about 2.7, and then only approaches the scaling solution value very slowly. Curves (b), (c) and (d) show the evolution of $1/\gamma^2$ with parameters for which no scaling solution exists, namely: $p_{sI} = 0.62$ and $F_L = 0.65, 0.55$ and 0.45 respectively. The point to emphasize here is that in all three of these graphs it looks as if $1/\gamma^2$ is approaching a constant if we see only the portion of the curves between $t = 1$ and about $t \approx 10$ that the numerical simulations are limited to. In each of these cases, however, the universe is doomed to become dominated by a mixture of cosmic strings and their gravitational radiation. Note that this occurs for a fairly large range in F_L .

Things are not so bad if δ is smaller or p_{sI} is larger. Then, the percentage of loops that reconnect is smaller and the transient behavior is less pronounced.

The transient is also reduced if the loop production function $a_2(x)$ is used for the same reason. Turok²⁴ claims that the most recent numerical results seem to indicate that there is significant loop production at very small sizes. This would indicate a fairly large value for p_{SI} . If this is confirmed, then this type of transient is not likely to be a serious problem although it still might contribute to errors in the measured value of ν .

The type of ambiguity that may be caused by a transient can be seen in somewhat more detail in Figs. 8 and 9 which are the analogs of Fig. 3 in Ref. 14. They give the energy density of all the strings with a radius greater than r (recall that $r = \ell/\sqrt{2}$) as a function of r . When the evolution is followed to times of order $30t_o$, both curves seem to approach a scaling solution. In reality, the string density in both figures continues to grow at later times. In Fig. 8, a scaling solution does exist so the only effect of the transient is to reduce the string density at early times. This will give rise to errors in the values for $1/\gamma^2$ and ν as determined by the numerical simulations at early times. The slope of these graphs can be used to calculate the value of the loop density parameter ν (see Eq. (3.2)) with the formula, $\nu = \frac{\text{slope}}{4\pi}$. From Fig 8, we can see that for $p_{SI} = 0.81$ attempting to calculate ν at times as early as $3t_o$ or $6t_o$ can easily give an error of a factor of 2 or 3. In Fig. 9, the apparent approach to a scaling solution is completely misleading because no scaling solution exists in this case.

It should be mentioned that there is one substantial difference between Figs. 8 and 9 and the corresponding graphs that can be obtained from the numerical simulations. Figs. 8 and 9 include only non-self-intersecting loops because I have taken loop fragmentation to occur instantaneously. The simulations, of course, also include loops that have not yet completed fragmenting. So, it is not

entirely straightforward to compare these graphs to the numerical simulations. Nevertheless, the figures should coincide with the simulations for small loops, so there is some correspondence between Figs. 8 and 9 and the simulations.

It should also be emphasized that the transient behavior discussed in this section is strongly dependent on the parameters δ and p_{sl} (or N_l) which control the efficiency of the loop production process. If the parameters are taken so that loop reconnection is very much suppressed, and the loop production efficiency is ≈ 1 , then both γ and ν evolve to the scaling solution values fairly quickly. On the other hand, if the loop production efficiency is small, then this problem is even worse. Therefore, it is important to try and measure the efficiency of loop production in the numerical simulations in order check that a scaling solution has indeed been reached, and if so, to estimate the uncertainty of the results.

5. STRING EVOLUTION INTO THE MATTER DOMINATED ERA

In this section, the evolution of a system of strings will be investigated in the matter dominated era. The scaling solution in the matter dominated era is studied in Sec. 5.1, while the realistic case of the transition from radiation to matter domination is treated in Sec. 5.2.

5.1 SCALING SOLUTION IN THE MATTER DOMINATED ERA

It was originally pointed out by Kibble² that the scaling solution has a somewhat simpler form in the matter dominated era. If we neglect the gravitational

radiation terms in (2.11) and (2.12), then (2.11) becomes

$$f(x) = \frac{p\bar{v}}{\gamma} \int_x^\infty dy a(y) \frac{y}{x} e^{p\bar{v}\delta(x-y)/\gamma}, \quad (5.1)$$

and the constraint (2.12) becomes

$$\frac{1}{3}(1 - 2\langle v^2 \rangle) = \frac{p\bar{v}}{2\gamma} \int_0^\infty dx a(x) e^{-p\bar{v}\delta x/\gamma}. \quad (5.2)$$

When x is sufficiently small, we can approximate the integral in (5.1) by taking the lower limit of integration to be 0. This makes the integrals in Eqs. (5.1) and (5.2) identical allowing them to be eliminated so that

$$f(x) = \frac{2}{3}(1 - 2\langle v^2 \rangle) \frac{e^{p\bar{v}\delta x/\gamma}}{x}, \quad \text{for small } x. \quad (5.3)$$

x is considered to be “sufficiently small” when

$$\int_0^x dy y a(y) \ll \int_0^\infty dy y a(y). \quad (5.4)$$

Since I have also implicitly assumed that $x \gg \epsilon$, it is quite possible to have loop production functions for which (5.3) is never a very good approximation. For $G\mu = 10^{-6}$, this occurs for $p_{SI} > 0.9$. For $p_{SI} \lesssim 0.8$, however, it is not too bad.

Just as in the radiation dominated era, it is convenient to define a loop density parameter,

$$\sigma_m \equiv x f(x), \quad (5.5)$$

that scales out the asymptotic x dependence. The matter era analog of Fig. 1 is Fig. 10 which is a plot of σ_m as a function of ℓ/t for different values of p_{SI} . The

other parameters are fixed at exactly the same values as those in Fig. 1 except that $k = 1/5$. Note that σ_m is constant over a large range of ℓ/t only when p_{sI} is fairly small unlike σ in Fig. 1. This is because the condition (5.4) does not hold for a large range in x when p_{sI} is large.

From (5.3) it is clear that in the matter dominated era the energy density of the strings is no longer dominated by the smallest loops. Instead, there is roughly an equal energy density in every logarithmic interval of loop size. The total energy density only depends logarithmically on the minimum size of the loops ($\ell_o \approx 10G\mu$). This means that in a matter dominated universe, the total string energy density scales as $\log(G\mu) G\mu$ rather than $(G\mu)^{1/2}$ which is the case during radiation domination.

Although the evolution equations are simpler in the matter dominated era, it is actually more difficult to study the scaling solution in the matter dominated era because we can no longer assume that $\langle v^2 \rangle \simeq \frac{1}{2}$. From Eq. (5.2), we can see that if $\langle v^2 \rangle$ were $\frac{1}{2}$, then the right hand side of (5.2) would have to vanish implying that $a(x) = 0$. But, we know that $a(x)$ must be rather large in the radiation dominated era so that the long strings can lose energy fast enough to allow $\rho_{LS} \sim 1/R^4$. In the matter dominated era, this energy loss mechanism must be balanced by the stretching of the strings, and this implies that $\langle v^2 \rangle \neq \frac{1}{2}$. We can no longer get away with assuming that string stretching is negligible because it is the only energy increasing process available to balance the energy loss through loop production. Thus, in order to solve for a scaling solution in a universe is dominated by nonrelativistic matter, it is necessary to have a reasonable form for $\langle v^2 \rangle$ as a function of γ .

Unfortunately, without further numerical simulations, it is difficult to make

any quantitative statements about $\langle v^2 \rangle$. Some qualitative statements can be made, however. It is clear from energy conservation that the scale length of the strings in the matter dominated era (γ_m) must be significantly greater than the scale length during the radiation dominated era (γ_r), so the value of $\langle v^2 \rangle$ must be significantly smaller. It can also be shown that if $\langle v^2 \rangle$ is a reasonably steep function of γ , then the value of $\gamma = \gamma_m$ at the scaling solution depends strongly on the form of $\langle v^2 \rangle$ but only weakly on the other parameters such as δ and p_{SI} . For instance, if I use (3.15), then $k = 1/16 \Rightarrow \gamma_m \approx 1.5$, $k = 1/5 \Rightarrow \gamma_m \approx 1.3$, and $k = 1/2 \Rightarrow \gamma_m \approx 1.0$.

5.2 STRING EVOLUTION DURING THE TRANSITION TO MATTER DOMINATION

When we study the evolution of strings in the radiation dominated era it is generally only necessary to study the behavior of the scaling solution. This is because we are generally interested in studying the strings a long time after t_0 (the time when they begin to move freely). So the strings have enough time to evolve to a scaling solution before we have any interest in them. In contrast, we are interested in string evolution at the very beginning of the matter dominated era because this is when the loops that are expected to be responsible for the formation of clusters of galaxies are formed. Therefore it is important to understand the behavior of strings during the transition period in some detail.

This can be accomplished through numerical integration of the evolution equations using the method given by Eqs. (2.15) and (2.16). First, we need the solution of Einstein's equation that describes the transition. The solution for a

universe with both matter and radiation ($\rho \sim (R + R_{eq})/R^4$) is

$$\frac{t}{t_{eq}} = \frac{1}{2 - \sqrt{2}} \left[\left(\frac{R}{R_{eq}} \right) \sqrt{\frac{R}{R_{eq}} + 1} + 2 \right]. \quad (5.6)$$

This can be inverted by the standard formulas for solving cubic equations to yield a (very messy) analytic expression for $R(t)$.

With (5.6) and its inverse, (2.15) and (2.16) can now be iterated numerically through the transition to the matter dominated era. I have done this calculation for 93 different sets of parameters, starting with a scaling solution at $t = 10^{-5} t_{eq}$ and running until $t \approx 10^6 t_{eq}$. The parameters were chosen to have values that seem to be consistent with the results of the numerical simulations. The following ranges of parameters were used: $0.46 \leq \gamma_r \leq 0.76$, $0.66 \leq p_{SI} \leq 0.94$, $4 \leq N_t \leq 20$, $0 \leq \delta \leq 0.7$, and $0.02 \leq k \leq 0.5$. In addition, several runs were done with $\langle v^2 \rangle$ given by functions other than (3.15).

My results for $\gamma(t)$ can be summarized with the following analytic fit,

$$\gamma = \frac{\gamma_m (t/t_*)^\zeta + \gamma_r}{(t/t_*)^\zeta + 1}. \quad (5.7)$$

This expression fits the numerical results remarkably well; the rms error was less than 0.5% in each of the 93 runs. It is also somewhat remarkable that all of the parameters in (5.7) can be determined to a reasonable accuracy if we know only the scaling solution values for γ in both the radiation era and the matter era. [These are γ_r and γ_m respectively.] ζ turns out to be almost independent of the input parameters with a mean value of $\bar{\zeta} = 0.47$ with a variation of at most 10%. Deviations from $\bar{\zeta}$ of 10% occur only at the boundaries of the parameter

space that has been explored. The variation in t_* can be given by the following expression,

$$\ln \left(\frac{t_*}{t_{eq}} \right) = \frac{1}{\zeta} [0.78 + 2.93(\gamma_m - \gamma_r) - 0.65(\gamma_m^2 - \gamma_r^2)] . \quad (5.8)$$

The maximum error from this expression is about 5% for $\ln(t_*/t_{eq})$ or 20% for t_* .

The fact that $\gamma(t)$ is essentially independent of all the parameters except for γ_r and γ_m seems to indicate that the time scale of the string system's response to the change in expansion rate is much slower than the change in the expansion rate. This means that during the transition, the strings are very far from the type of equilibrium that characterizes a scaling solution. This also explains why the time when the strings are midway through their transition, t_* , tends to be roughly a factor of 50 greater than t_{eq} . $\dot{\gamma}(t_*)$ is roughly the same as it would be if $R(t)$ changed discontinuously from $R \sim t^{1/2}$ to $R \sim t^{2/3}$. If $\langle v^2 \rangle \approx \frac{1}{2}$, then from Eq. (2.7) we get $\dot{\gamma} = \gamma/4t$ when R changes discontinuously. This is nearly identical to the result obtained from Eq. (5.7) at $t = t_*$: $\dot{\gamma}(t_*) = \zeta/2t$.

My results for $f(t, x)$ can also be summarized with an analytic fit,

$$f(t, x) = \frac{e^{-\alpha x}}{x} \left(\frac{\Sigma}{1 + At^q} \frac{1}{x^{1/2}} + \Sigma_m \right) . \quad (5.9)$$

This fit typically has an rms error of about 10%. The parameters Σ and Σ_m are to be identified with the loop density parameters σ and σ_m introduced in the previous discussion of the scaling solutions. Σ and Σ_m are to be considered to be constants rather than slowly varying functions of x like σ and σ_m . The best values for these parameters are obtained by setting $\Sigma = \sigma(x = 10^{-2})$ and $\Sigma_m = \sigma_m(x = 10^{-4})$.

The parameter q is a constant independent of the input parameters to a good approximation. Only at the edges of the parameter range does the deviation of q from $\bar{q} = 0.47$ approach 10%. It is not difficult to understand why $q \approx \frac{1}{2}$. Since small loops obey $\rho_{\text{loops}} \sim R^{-3}$ just like nonrelativistic matter, the density of loops with a fixed size ℓ should just scale like t^{-2} in the matter dominated era (assuming that loop production at the scale of ℓ is small). In the expression for the energy density, (2.5), it can be seen that the prefactor of t^{-2} is carried by the factor E/V so that $f(x) dx$ should be independent of time. Since $x = \ell/\gamma t$, the expression (5.9) can be made independent of t for small x and large t only by setting $q = \frac{1}{2}$. Thus, (5.9) seems to have the basic properties that we expect of it at small x : $f(t, x) \sim \sigma x^{-3/2}$ in the radiation era, and $f(t, x) \sim \sigma_m x^{-1}$ well into the matter dominated era. It also has a term proportional to $t^{-1} x^{-3/2}$ to describe the behavior of loops that form during radiation domination, but that survive into the matter era.

Unfortunately, there are no such simple interpretations for the parameters A and α . The parameter A was found to be roughly $A = 0.18 \pm 0.06$ where the range of values for A corresponds to the range of parameter space that has been explored. In general, A seems to be a function of $p_{s\ell}$ (or N_ℓ), δ , and k . It tends to be largest when loop reconnection is very much suppressed. The parameter, α is included to take into account the falloff of $f(x)$ at $x \sim 1$. In fact, it does not provide a particularly good fit with either loop production function. However, since the model assumes that loop fragmentation takes place instantaneously, there is no reason to expect that the model would give the right values for $f(x)$ near $x \sim 1$ anyway. With the loop production function $a_1(x)$, the typical value for α was around 2. With $a_2(x)$, a θ -function cutoff $\theta(1/N_\ell - x)$, should be

understood to multiply Eq. (5.9). With this cutoff, higher values for α were possible depending on the value of N_ℓ . For $N_\ell = 10$, the typical value of α was about 4.

6. SUMMARY AND CONCLUSIONS

I have extended the study presented in (I) of the evolution of a system of cosmic strings using an analytic formalism based on the work of Kibble.² The scaling solution that is expected to describe string evolution in the radiation dominated era has been studied in great detail. The results of this analysis are summarized in Table 1 which gives approximate analytic formulas for the loop density parameter σ as a function of the loop reconnection factor δ and the probability of self-intersection (represented by p_{SI} or N_ℓ depending on which loop production function is used). This formula for σ can easily be translated into a formula for the number density of small loops in terms of δ , p_{SI} (or N_ℓ), and γ . The results for the small loop density seem to be in conflict with the loop density obtained in the numerical simulations of Albrecht and Turok by a factor of ~ 3 (assuming $p_{SI} \leq 0.85$ or $N_\ell \leq 10$). This discrepancy does not depend of the form of the loop production function or any of the parameters in the model except for p_{SI} and N_ℓ . Albrecht and Turok's value can be obtained only when the typical child loop size is very small *i.e.* if $p_{SI} \simeq 0.95$ or $N_\ell \simeq 60$. Turok has suggested that such small loops may actually be seen in the simulations; however, the data from the simulations is not yet sufficient to confirm this.

In Sec. 4, I tried to look for possible systematic errors in the numerical simulations that may result from their initial conditions. My approach was to solve Kibble's evolution equations numerically starting from an initial condition

similar to that used by Albrecht and Turok. It was shown that the loop density can be underestimated by a factor as large as 2 or 3 when it is measured at $t = 3t_0$ as Albrecht and Turok have done. If $p_{SI} < 0.7$, the lack of small loops in the initial state used for the numerical simulations can lead to very deceptive results. With these parameters, I have shown that the string system can have a transient behavior that mimics relaxation to a scaling solution. Eventually, this transient behavior disappears and string density begins to grow, but this may only occur on a time scale which is longer than the simulations can be run. The correct value for p_{SI} seems to be greater than 0.7, so this type of transient may be unphysical. However, we will probably have to wait until the numerical results have been closely fit to an analytic model before we can be sure of this.

The upper bound on $G\mu$ that comes from the primordial nucleosynthesis limit on the energy density of gravitational radiation has been calculated in somewhat more detail than in (I), and I have shown how this bound depends on the parameters and assumptions of the model. I have emphasized that this upper bound, $G\mu \lesssim 4 \times 10^{-6}$, is inconsistent with claims that objects that are gravitationally lensed by cosmic strings will have a typical separation of an arc minute or more.

Finally, I have followed the evolution of the string system into the matter dominated era by integrating the evolution equations. Although the density of long strings at the matter era scaling solution remains to be found by numerical simulations, it clearly must be much less than the density in the radiation era. My calculations of string evolution through the transition from radiation domination to matter domination show that the transition probably takes much too long to be handled by a numerical simulation. Fortunately, the behavior of the string

system can be described fairly accurately by analytic fits to my results. The free parameters in these analytic formulas can be almost completely determined from the scaling solutions in both the radiation and the matter dominated eras.

The next step in the study of cosmic strings must be to do a detailed analysis of the numerical simulations with an analytic model such as the one invented by Kibble which has been developed here. Without help from the numerical simulations, we are left with a large number of unknown parameters, so it is difficult to make any firm predictions with the analytic model alone. Similarly, if we rely on only the numerical simulations, we can never be sure that the simulations are not being influenced by some unknown systematic problem. Thus, probably the only way to solve the problem is to fit all the free parameters of the analytic model directly from the simulations.

ACKNOWLEDGEMENTS

I would like to thank J. Primack, A. Vilenkin, A. Albrecht, N. Turok and H. Quinn for helpful discussions.

REFERENCES

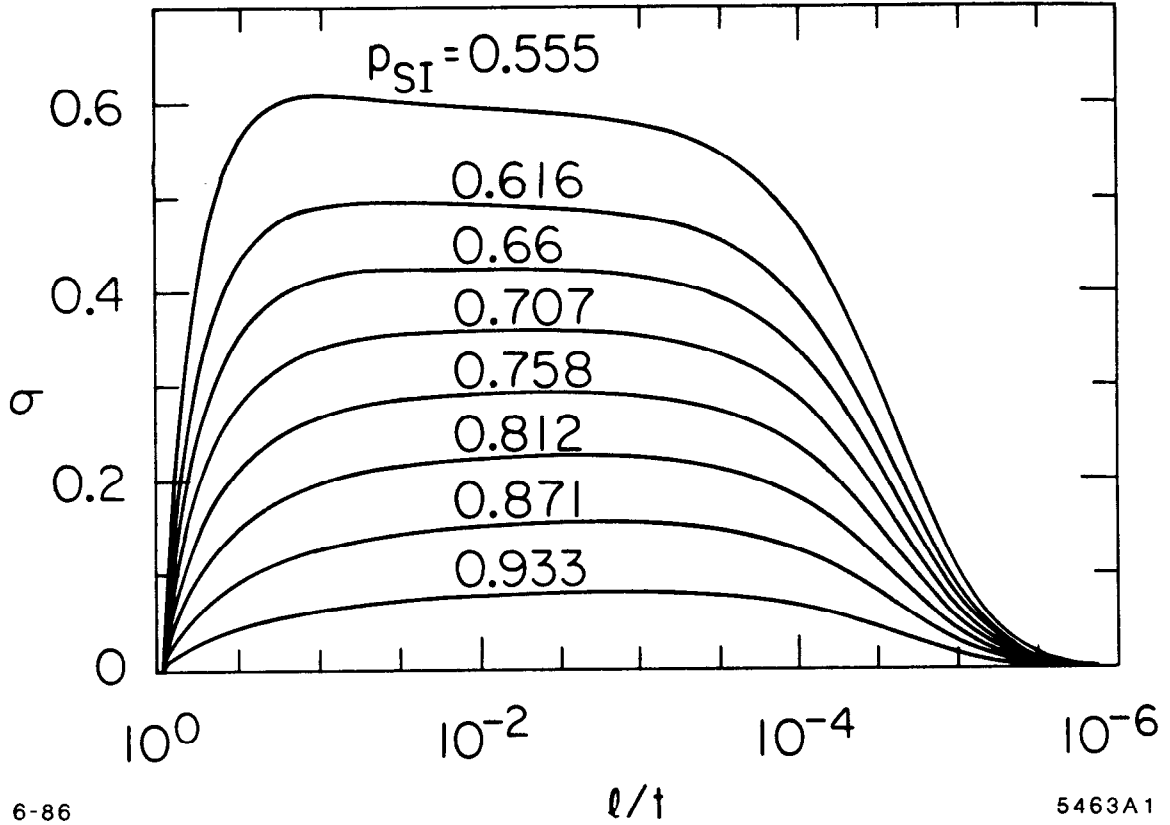
1. D. P. Bennett, *Phys. Rev.* **D33** (1986) 872; Erratum to be published.
2. T. W. B. Kibble, *Nucl. Phys.* **B252** (1985) 227
3. N. Turok and P. Bhattacharjee, *Phys. Rev.* **D29** (1984) 1557
4. A good review of cosmic strings is A. Vilenkin, *Phys. Rep.* **121** (1985) 263
5. Y. B. Zel'dovich, *Mon. Not. R. Astron. Soc.* **192** (1980) 663
6. A. Vilenkin, *Phys. Rev. Lett.* **46** (1981) 1169
7. A. Vilenkin and Q. Shafi, *Phys. Rev. Lett.* **51** (1983) 1716
8. N. Turok, *Nucl. Phys.* **B242** (1984) 520
9. J. Silk and A. Vilenkin, *Phys. Rev. Lett.* **53** (1984) 1700
10. N. Turok and D. N. Schramm, *Nature* **312** (1985) 598
11. N. Turok, *Phys. Rev. Lett.* **55** (1985) 1801
12. N. Turok and R. Brandenberger, *Phys. Rev.* **D33** (1986) 2175
13. A. Stebbins, *Astrophys. J.* **303** (1986) L21
14. A. Albrecht and N. Turok, *Phys. Rev. Lett.* **54** (1985) 1868
15. T. W. B. Kibble, *Phys. Rev.* **D33** (1986) 328
16. A. M. Boesgaard and G. Steigman, *Ann. Rev. Astron. Astr.* **23** (1985) 319;
J. Yang, M. S. Turner, G. Steigman, D. N. Schramm, and K. A. Olive, *Ap. J.* **281** (1984) 493
17. R. L. Davis, *Phys. Lett.* **161B** (1985) 285

18. R. H. Brandenberger, A. Albrecht, and N. Turok, DAMTP preprint, "Gravitational Radiation from Cosmic Strings and the Microwave Background", 1986
19. P. Paczynski, *Nature* **319** (1986) 567
20. J. R. Gott, *Nature* **321** (1986) 420
21. P. Shellard, Ph.D. Thesis, unpublished
22. T. Vachaspati and A. Vilenkin, *Phys. Rev.* **D30** (1984) 2036
23. C. J. Burden, *Phys. Lett.* **164B** (1985) 277
24. N. Turok, private communication
25. A. E. Everett, *Phys. Rev.* **D24** (1981) 858
26. S. Weinberg, *Gravitation and Cosmology: Principles and Applications of the General Theory of Relativity*, (New York, Wiley, 1972).
27. G. Lazarides, C. Panagiotakopoulos, and Q. Shafi, *Phys. Rev. Lett.* **56** (1986) 432
28. E. L. Turner, *et al.* *Nature* **321** (1986) 142
29. P. A. Shaver & S. Christiani, *Nature* **321** (1986) 585
30. A. Vilenkin, *Astrophys. J.* **282** (1984) L51
31. J. R. Gott, *Astrophys. J.* **288** (1985) 422
32. J. Frieman in *Inner Space Outer Space* proceedings, (eds. E. W. Kolb, M. S. Turner, D. Lindley, K. Olive, & D. Seckel), 540, (University of Chicago Press, Chicago, 1986).
33. N. Kaiser & A. Stebbins, *Nature* **310** (1984) 391
34. A. Albrecht, private communication

FIGURE CAPTIONS

1. The loop density parameter, σ vs. loop size ℓ/t using the loop production function $a_1(x)$ with $\xi = 1.5$, $\gamma = 1/\sqrt{2.5}$ and $\delta = 0.5$.
2. The loop density parameter, σ vs. loop size ℓ/t using the loop production function $a_2(x)$ with $\gamma = 1/\sqrt{2.5}$ and $\delta = 0.5$.
3. The loop production efficiency is plotted as a function of p_{SI} for the loop production function $a_1(x)$ (solid lines) and for $a_2(x)$ (dotted lines). [The relationship between $a_2(x)$ and p_{SI} is given in eq. (3.16).]
4. Contour plot for the bound on $G\mu$ due to nucleosynthesis constraints on the density of gravitational radiation (using $a_1(x)$) as a function of p_{SI} and $1/\gamma^2 = \rho_{LS}t^2/\mu$.
5. Contour plot for the bound on $G\mu$ due to nucleosynthesis constraints on the density of gravitational radiation (using $a_2(x)$) as a function of N_ℓ and $1/\gamma^2 = \rho_{LS}t^2/\mu$.
6. The density of loops (with a factor of $\ell^{-3/2}$ scaled out), σ/γ^2 vs. the loop size ℓ/t for different times as the scaling solution is approached from an initial condition with $f(t_o, x) = 0$, $p_{SI} = 0.81$ and $\delta = 0.5$.
7. The density of long strings, $1/\gamma^2 = \rho_{LS}t^2/\mu$ is plotted as a function of time from an initial state without small loops for the following parameters: (a) $p_{SI} = 0.81$ and $F_\ell = 0.47$. (b) $p_{SI} = 0.62$ and $F_\ell = 0.65$. (c) $p_{SI} = 0.62$ and $F_\ell = 0.55$. (d) $p_{SI} = 0.62$ and $F_\ell = 0.45$. In all graphs, $\delta = 0.5$.
8. Energy density of loops with radii greater than r , $\rho_r\mu/t^2$ vs. $(2t/r)^{1/2}$ at selected times starting with $f(t_o, x) = 0$ for $p_{SI} = 0.81$ and $\delta = 0.5$ as in Fig 7(a).

9. Energy density of loops with radii greater than r , $\rho_r \mu / t^2$ vs. $(2t/r)^{1/2}$ at selected times starting with $f(t_0, x) = 0$ for $p_{SI} = 0.62$ and $\delta = 0.5$ as in Fig 7(b).
10. The loop density parameter for the matter dominated era, σ_m vs. loop size ℓ/t using the loop production function $a_1(x)$ with $\xi = 1.5$, $\gamma_r = 1/\sqrt{2.5}$, $k = 1/5$ and $\delta = 0.5$.

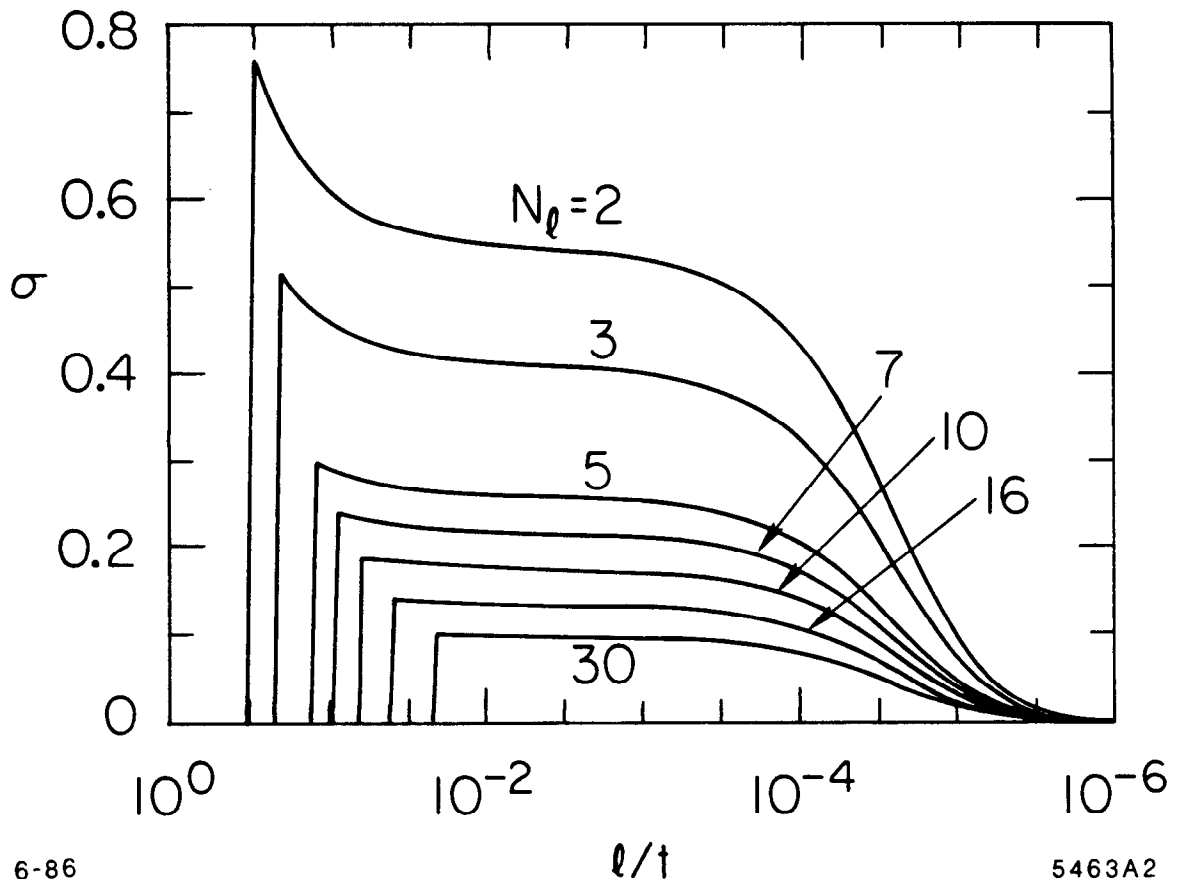


6-86

l/t

5463A1

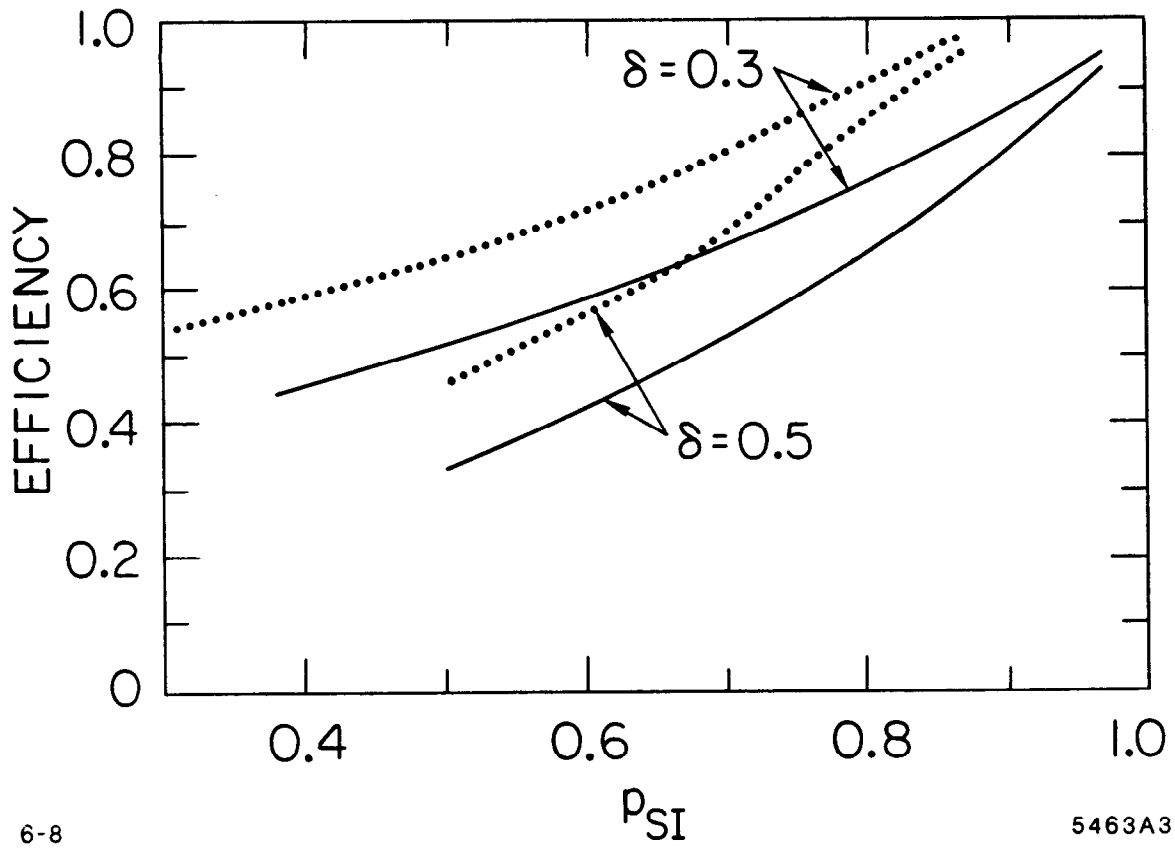
FIG. 1



6-86

5463A2

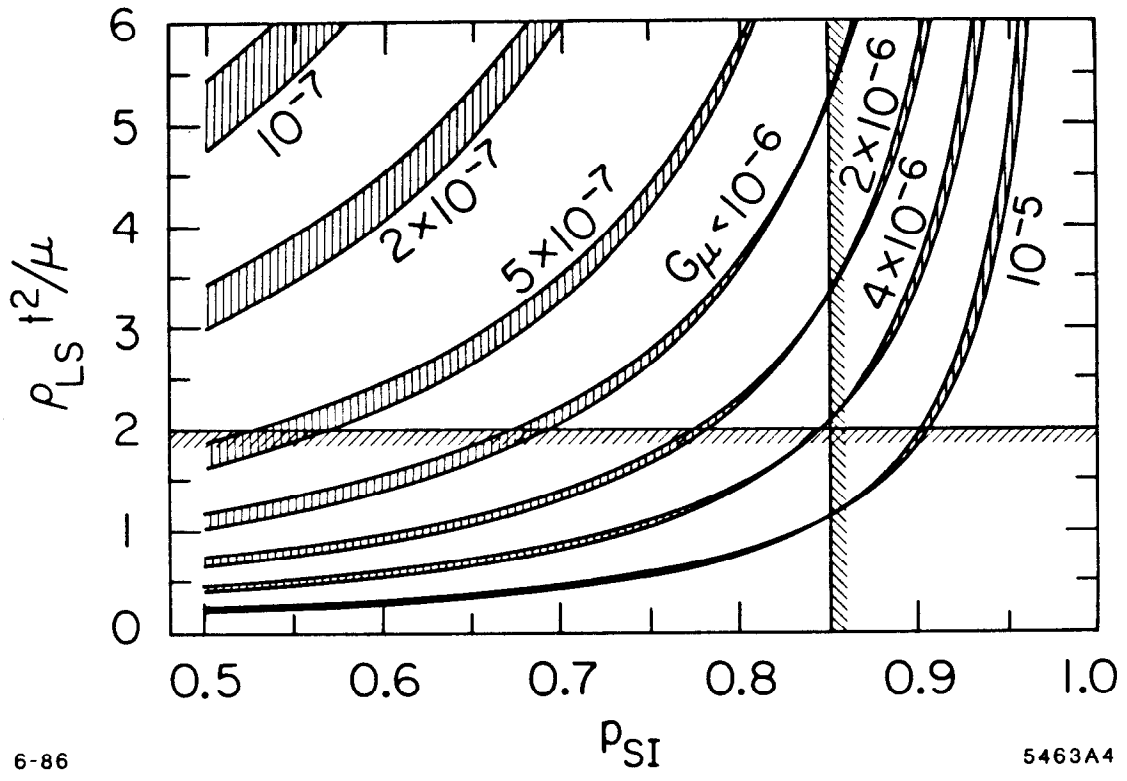
FIG. 2



6-8

5463A3

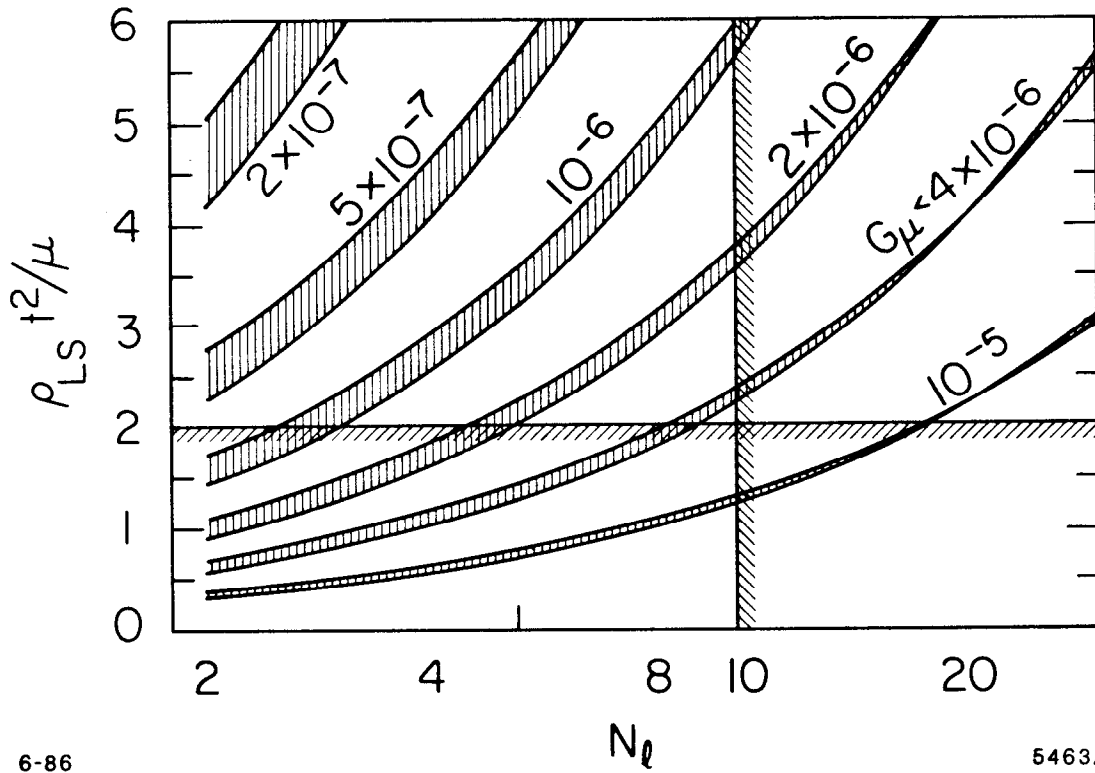
FIG. 3



6-86

5463A4

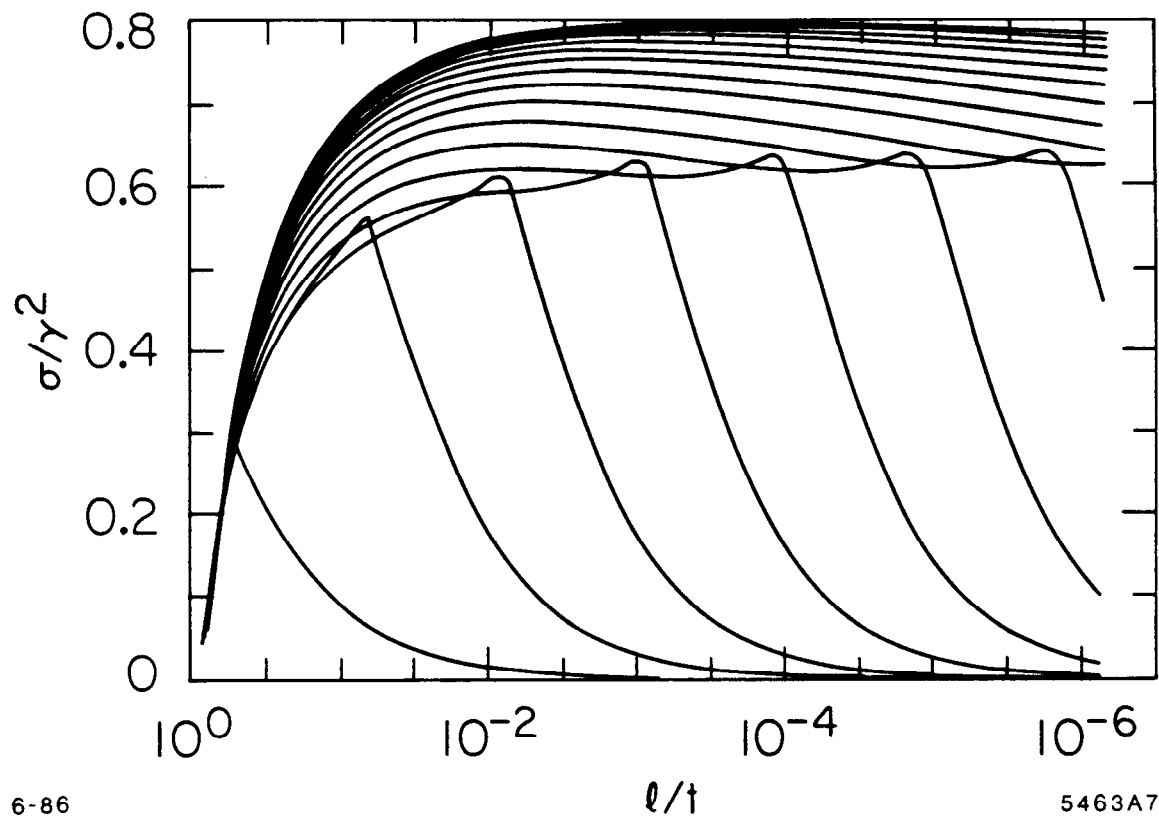
FIG. 4



6-86

5463A5

FIG. 5



6-86

l/t

5463A7

FIG. 6

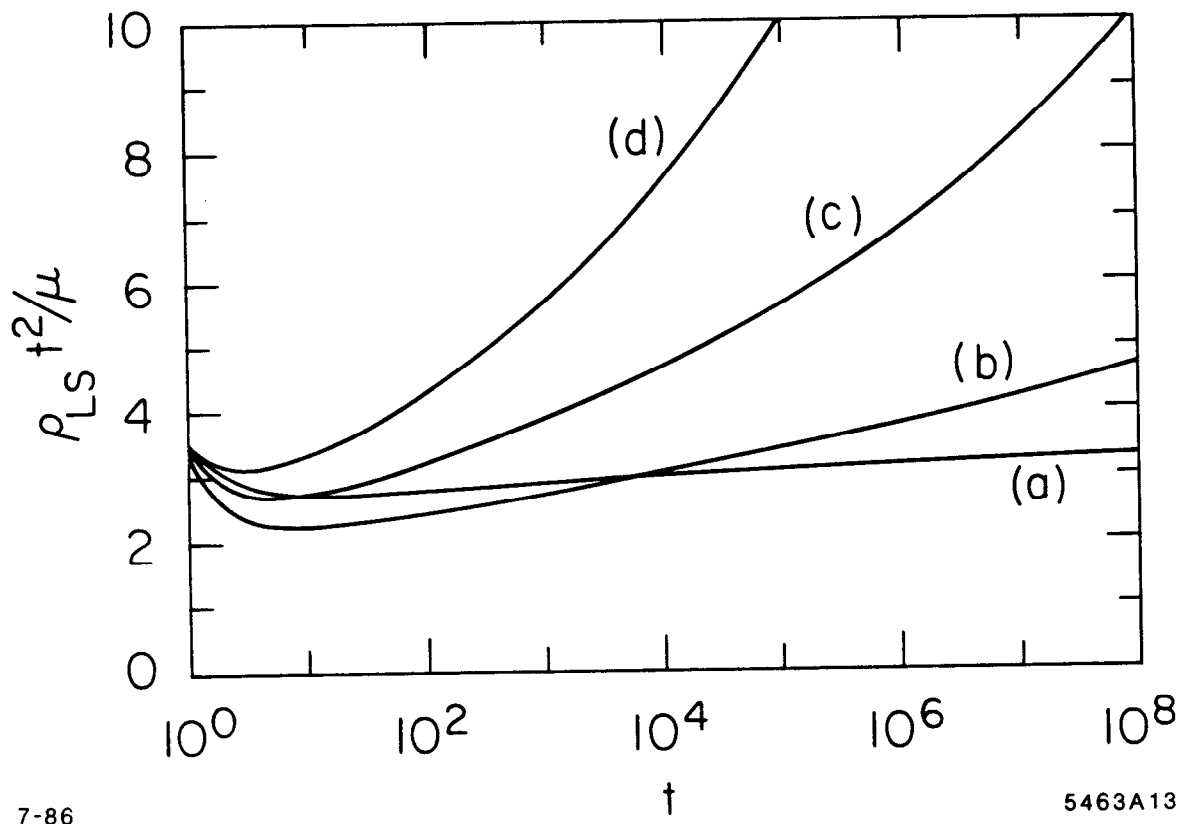
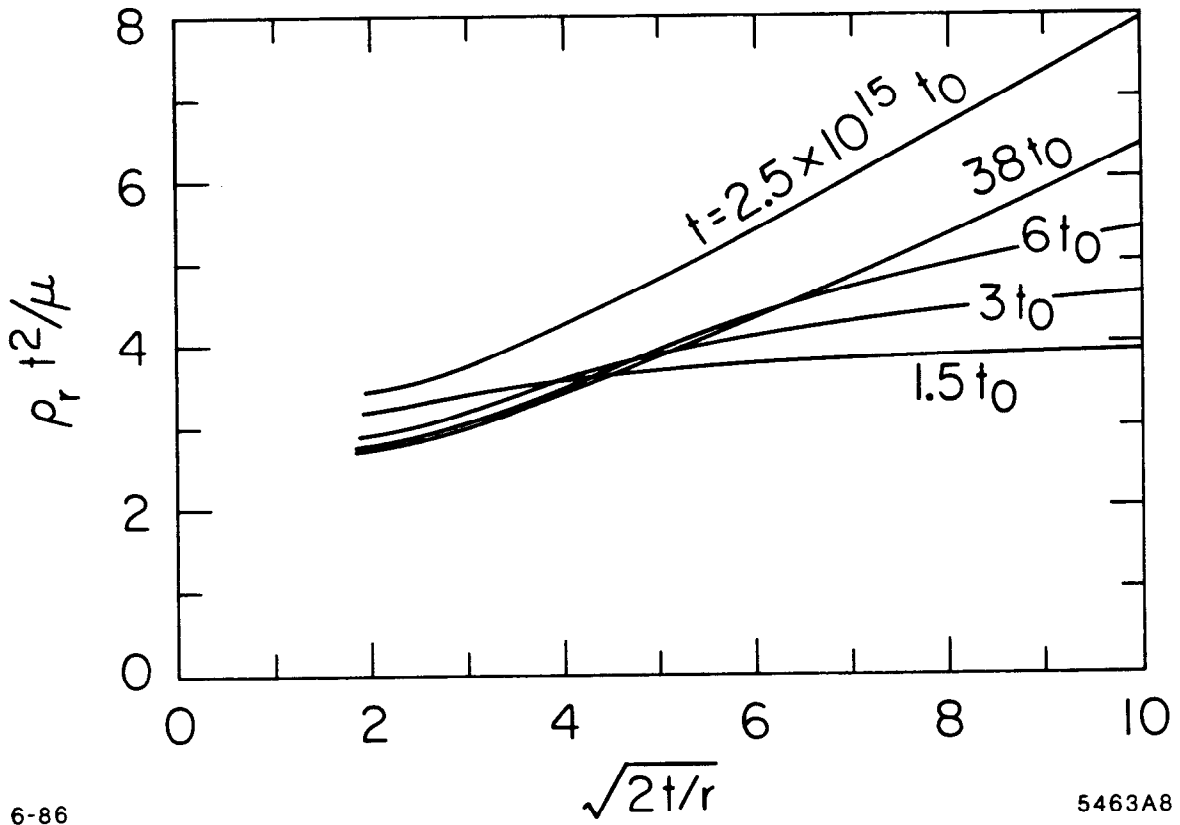


FIG. 7



6-86

5463A8

FIG. 8

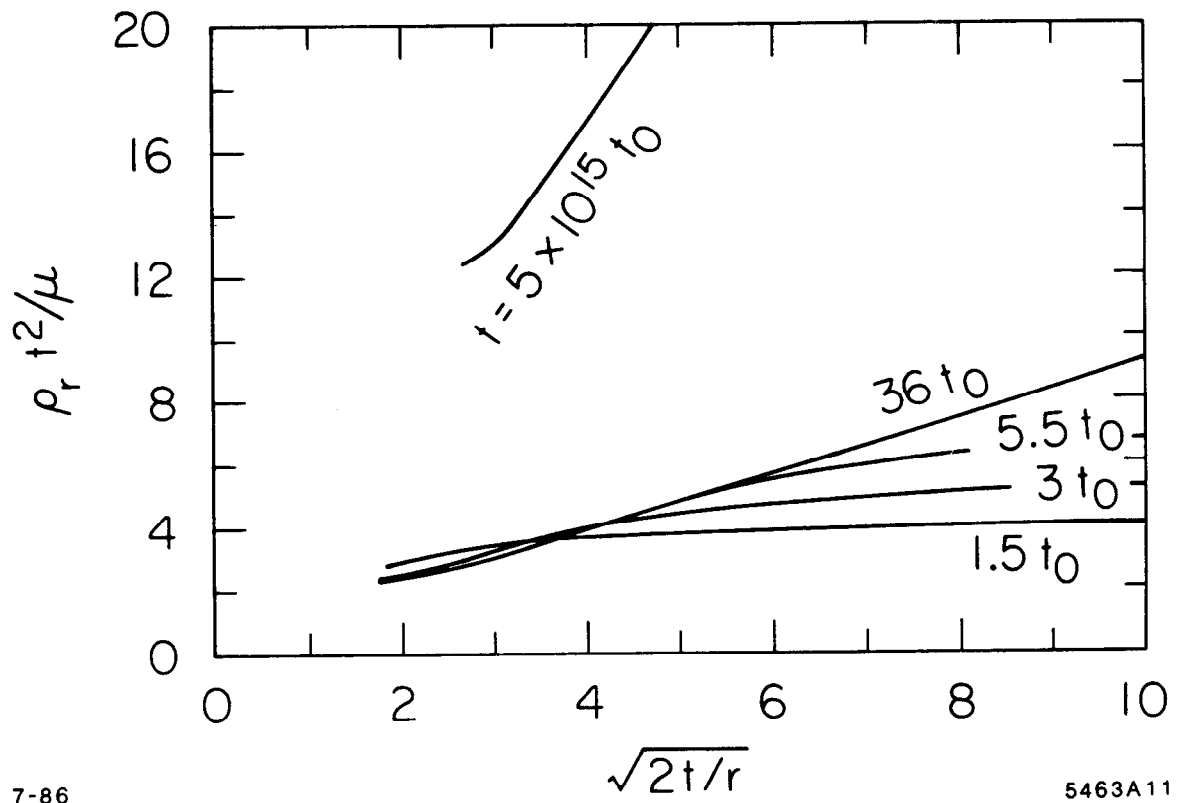


FIG. 9

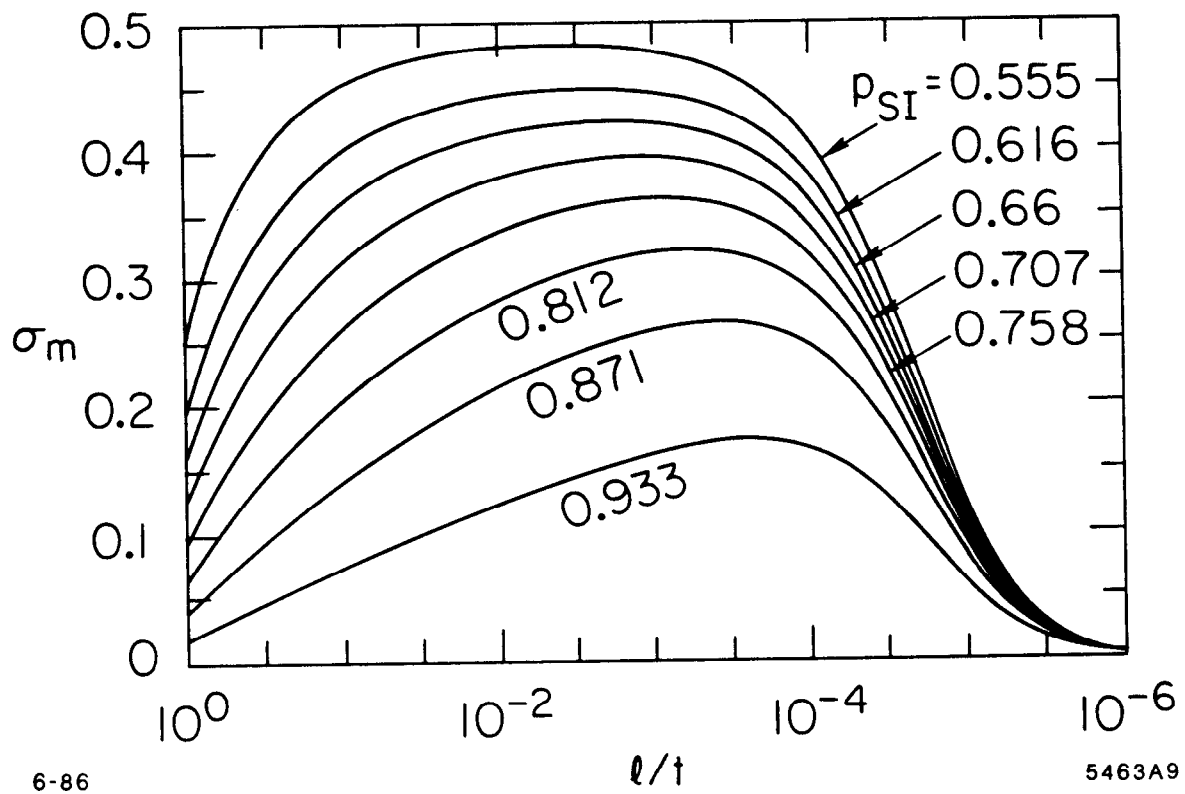


FIG. 10